

**New Approaches to Determining Shortest Cutters and Work  
Piece Setups without Over-travel for 5-axis CNC Machining**

**Aqeel Ahmed**

A Thesis in the Department

of

Mechanical and Industrial Engineering

Presented in Partial Fulfillment of the Requirements

For the Degree of Doctor of Philosophy (Mechanical Engineering) at

Concordia University

Montreal Quebec, Canada

September 2013

© Aqeel Ahmed, 2013

**CONCORDIA UNIVERSITY**  
**SCHOOL OF GRADUATE STUDIES**

This is to certify that the thesis prepared

By: **Aqeel Ahmed**

Entitled: **New Approaches to Determining Shortest Cutters and Work Piece  
Setups without Over-travel for 5-axis CNC Machining**

and submitted in partial fulfillment of the requirements for the degree of

DOCTOR OF PHILOSOPHY (Mechanical Engineering)

complies with the regulations of the University and meets the accepted standards with respect to originality and quality.

Signed by the final examining committee:

_____	Chair
Dr. G. Butler	
_____	External Examiner
Dr. D. Xue	
_____	External to Program
Dr. Y. Zeng	
_____	Examiner
Dr. M. Y. Chen	
_____	Examiner
Dr. A. Akgunduz	
_____	Thesis Supervisor
Dr. C. Chen	

Approved by \_\_\_\_\_  
Dr. A. Dolatabadi, Graduate Program Director

September 6, 2013

\_\_\_\_\_  
Dr. C. Trueman, Interim Dean  
Faculty of Engineering & Computer Science

# **ABSTRACT**

New Approaches to Determining Shortest Cutters and Work Piece Setups without Over-travel for 5-axis CNC Machining

Aqeel Ahmed, Ph.D.

Concordia University, 2013

Five axis CNC machining centers are widely used in the industries for producing the complex parts. Due to two more axes as compared to the three axes machining, it provides the efficient and flexible way of the machining. Besides this flexibility, accidental collision possibilities between the cutting system and the other moving parts of the machine tools are also increased. These collisions could be avoided by changing the orientations of the tool during the tool path planning or by adjusting the cutter length and the tool holder size after the tool path generation in the part coordinate system. Collision detection and removal by the optimum cutter length depends on the configuration of five axis machine tools. No. of possible candidates for the collision may vary with the configuration of the machine tools. Since the fully utilization of the existing machining facilities in the industry is also in high demand, therefore, after selecting the one of the critical parameter of the cutter length, the maximum utilization of the work space of the 5-axis machine tools is another critical task.

This dissertation comprises of two main works.

In the first research work, a comprehensive approach for the determination of the optimum cutter length for the specific configuration of five axis machine tool is developed. The complete cutting system (the tool, the tool holder and the spindle), the work in process model and the fixture are the three possible candidates for the collision. The work in process model and the fixture are represented as the point cloud data and the tool holder and the spindle are represented as a regular shape of the truncated cone and the cylinder respectively. Collision checking is conducted in two steps. In the first step the KD-tree data structure is employed on the point cloud data and a method is developed which confines the searching of the point cloud data in the local region and in the second step a new mathematical model for the collision detection between the points in the local region and the cutting system is established. This model also has the capability of removal collision with the optimum cutter length.

In the second research work, kinematics of the table rotating and spindle tilting 5-axis machine is developed and setup parameters for mounting the part on the table are defined. A precise method for the determination of the setup parameters, which gives the opportunity of fully utilization of the work space of the machine tool, is developed. Many machining simulation software such as vericut can simulate the G-codes for the given setup parameters of the part and can verify the over travel limits of the machine tool as well as accidental collision between the moving parts of the machine. In this research, the developed method for the determination of the setup parameters gives the guarantee of complete machining of the part without over travel limits of the machine translational axes. This research is based on the predetermined machining strategies, which means, tool path is already given in the part coordinate system.

# Dedication

*To my parents, father and mother in law, wife and kids*

# ACKNOWLEDGEMENTS

I would like to express my special thanks to my supervisor Prof. Chevy Chen for his sincere help, advices and support to achieve the milestones of my PhD work. Under his supervision I have gained precious research experience and significantly improved my technical skills.

I also want to give thanks to my current and the former fellow graduate students in our CAD/CAM laboratory, for providing all sorts of help and creating an excellent working atmosphere. The assistance of the faculty and staff of the Mechanical and Industrial Engineering Department is also highly appreciated.

I would also like to acknowledge the financial and moral support of NED University of Engineering and Technology, Karachi, Pakistan

# Table of contents

List of figures.....	x
List of table.....	xiii
Chapter 1 .....	1
Introduction.....	1
1.1 Classification of 5-Axis machines.....	1
1.1.1 Configuration of DMU 60T 5-axis machine .....	3
1.1.2 Advantages and Disadvantages .....	4
1.2 Tool path generation .....	5
1.3 Post processing.....	7
Chapter 2 .....	9
Literature Review and Research Objectives .....	9
2.1 Literature review.....	9
2.1.1 Software overview .....	10
2.1.2 Literature review on collision detection.....	11
2.1.3 Literature review on post processing .....	13
2.2 Research problems and objectives.....	14
2.2.1 Identification of the research problems .....	14
2.2.2 Research objectives.....	16
Chapter 3 .....	19
A Comprehensive Approach to Determining Minimum Cutter Lengths for 5-Axis Milling.....	19
3.1 Types of collision in five axis machining .....	20
3.2 Cutting system model and point cloud representation of the in-process or the fixture model .....	20
3.2.1 Parametric CAD model of the cutting system .....	21
3.2.2 In-process work piece model.....	22
3.2.3 Point cloud generation .....	23
3.3 The interference free cutter length model.....	24

3.3.1	Spindle interference free cutter length model .....	25
3.3.2	Tool holder interference free cutter length model .....	26
3.4	The new search method for minimum cutter lengths .....	28
3.4.1	Two dimension Kd-tree data structure.....	28
3.4.2	Orthogonal range determination model for the spindle.....	30
3.4.3	Algorithm of the collision detection with the spindle (cylinder) and removal by the optimum tool length .....	32
3.4.4	Orthogonal range determination model for the tool holder .....	36
3.4.5	Algorithm of the collision detection with the tool holder (truncated cone) and removal by the optimum tool length.....	38
3.5	Applications .....	42
3.5.1	Determination of the possible candidate points for the collision detection by the KD tree approach.....	43
3.5.2	Results and simulation verification .....	45
3.6	Summary .....	48
Chapter 4	.....	49
	<b>A Precise Approach for the Determination of the Setup Parameters to Utilize the Maximum Work Space of 5-Axis Machine Tools .....</b>	<b>49</b>
4.1	Kinematics of the 5-axis machine tool.....	52
4.1.1	Derivation of the machine translational coordinates.....	54
4.1.2	Machine tool rotations.....	56
4.2	Tool tip accessible work space model .....	57
4.2.1	Unsymmetrical spindle rotation limits.....	58
4.2.2	Rectangular tool tip range in the table coordinate system.....	59
4.3	Mathematical model for the determination of the feasible region on the table for mounting the work piece based on the tool tip accessible work space ...	61
4.3.1	Model for generating the polygon of the feasible region .....	64
4.4	Determination of the feasible ‘dz’ parameter of mounting the work piece on the table.....	69
4.5	Machining examples along with the simulation verification .....	71
4.5.1	Prismatic part machining with two machining processes .....	71
4.5.2	Prismatic part machining with multiple machining processes .....	74

4.5.3	Machining of the ‘bracket for holding the pipe’ .....	79
4.6	Summary .....	84
Chapter 5	.....	86
Conclusions and Future Work	.....	86
References	.....	88
Appendix A	.....	91
A.1:	Derivation of homogenous transformation matrix from cutter coordinate system to the work piece coordinate system “ $T_w^{cutter}$ ” .....	91
A.2:	Machine rotations (C and b) solutions for the given tool orientations ....	96

# List of figures

## Chapter1

Figure 1.1- Types of 5-axis milling machines: (a) Table-rotating/tilting type (b) Spindle-rotating /tilting type (c) Table/spindle –tilting type .....	2
Figure 1.2- Configuration of DMU 60T 5-axis milling machine .....	4
Figure 1.3-Tool path generation method research topics for 5-axis machining .....	6

## Chapter2

Figure 2.1-Detailed architecture of the research problems definition .....	16
--	----

## Chapter3

Figure 3.1- Possibility of the spindle collision with the fixture in actual machining environment .....	20
Figure 3.2- Cutting system profile in the cutter coordinate system .....	21
Figure 3.3- In process work piece model after roughing operation .....	22
Figure 3.4- Tessellated triangular representation of the in-process work piece model ....	23
Figure 3.5- (a) Triangular mesh surface (b) point cloud data with $D=0.5$ points/mm <sup>2</sup> .....	24
Figure 3.6- (a) Bisecting of the data points (b) Kd-tree data structure .....	29
Figure 3.7- Checking procedure for the orthogonal searching query .....	30
Figure 3.8- Flow chart of the algorithm for the spindle collision detection and removal by the optimum cutter length .....	35
Figure 3.9- Flow chart of the algorithm for the tool holder collision detection and removal by the optimum cutter length .....	41
Figure 3.10-(a) Solid model (b) Triangular tessellation representation. (c) Point cloud data representation of the work in process model along with the fixture in part coordinate system. ....	43
Figure 3.11-No. of points determined from the orthogonal range of spindle by Kd-tree structure of 30672 sample points, when tool length is 40mm. ....	44
Figure 3.12- No. of points determined from the orthogonal range of the tool holder by Kd-tree structure of 30672 sample points, when tool length is 56.4476mm. ....	45
Figure 3.13- At 3 <sup>rd</sup> tool path and 20 <sup>th</sup> cutter location with machine rotations of $C=-26.49^\circ$ $b=52.74^\circ$ (a)Collision of cutting system with the fixture and work in process model with tool length of 40mm. (b) No collision with the tool length of 56.45mm.....	46

Figure 3. 14-(a) At 2<sup>nd</sup> tool path and 18<sup>th</sup> cutter location with machine rotations of C=-223.477° and b=56.890° collision of the cutting system with the tool length of 40mm. (b) No collision with the tool length of 62.46mm and (c) At 20<sup>th</sup> cutter location with machine rotations of C=-232.22° b=49.15° collision of the cutting system with tool length of 40mm. (d) No collision with the tool length of 49.592mm. .... 47

## Chapter4

Figure 4.1- Standard setup parameters of a part on the machine table .....	50
Figure 4.2- Basic methodology for finding the feasible setup parameters. ....	51
Figure 4.3- (a) Transformation sequence along with the reference coordinate system. (b) Standard setup of the part on the machine table. ....	53
Figure 4.4- x and y travel limits in the table coordinate system ‘o <sub>t</sub> ’ .....	57
Figure 4. 5- (a) Unsymmetrical limits of spindle rotation & (b) Tool tip maximum range profile on the plane parallel to y <sub>t</sub> z <sub>t</sub> -plane. ....	59
Figure 4. 6- Rectangular range for the different values of the spindle rotation.....	60
Figure 4.7- Rectangular range at some value of the spindle rotation along with the setup parameters. ....	62
Figure 4.8- (a) Randomly named five vertices of the polygon. (b) Angles measured between the x-axis and the different vectors from the lower left point to the other vertices of the polygon (c) Points arrangement according the ascending order of the ‘θ’ (d) Final polygon. ....	66
Figure 4.9- No feasible region case when $FR_L \cap FR_p = \emptyset$ .....	67
Figure 4.10- No change in the feasible region when inequality function is applied or when $FR_L \cap FR_p = FR_p$ .....	68
Figure 4.11- Reduction in the feasible region when inequality function is applied or when $FR_L \cap FR_p = FR_p$ . ....	68
Figure 4.12- Table travel limit along with the machine constants d <sub>1</sub> and d <sub>2</sub> .....	70
Figure 4.13- (a) Design part with the rough stock. (b) Tool path generation snap shots .	72
Figure 4.14- (a) Feasible region for selecting the setup parameters. (b) Example of setup the part when setup parameters are selected within the feasible region .....	73
Figure 4.15- (a) Setup of the part when setup parameters are selected from outside the feasible region (b) Snap shot of the simulation showing that further machining is not possible due to the limitation of the x-travel .....	74
Figure 4.16-Design part and the rough stock.....	75
Figure 4.17-Snap shot of the top facing.....	75
Figure 4.18-Snap shot of the four corners inclined facing.....	76
Figure 4.19-Five feasible regions for five machining processes along with the final common feasible region. ....	77

Figure 4.20- Feasible setup of the part on the machine table along with the location of the feasible point inside the final feasible region .....	78
Figure 4.21- Infeasible setup of the part on the machine table along with the location of the feasible point outside the final feasible region.....	79
Figure 4.22-Design part (bracket for holding the pipe) and the rough stock.....	80
Figure 4.23- (a) Top surface facing (b) Pocketing of the four open islands (bottom faces) with three passes .....	81
Figure 4.24- (Snap shot contd.): (c) Five axis continuous machining of the top surface of the four supporting ribs with two levels (d) Profile contouring of the cylindrical surface and four edges (e) Drilling and internal pocketing.....	82
Figure 4.25- Common feasible region along with feasible regions for each machining operation. ....	83
Figure 4.26- (a) Feasible setup of the rough stock. (b) Infeasible setup parameters of the rough stock.....	84

### ***Appendix A***

Figure A1- Configuration of DMU 60-T along with the reference coordinate systems...	91
Figure A2- (a) & (b) Positive rotation of the table ‘C’ for positive rotation of spindle ‘b’, when tool vector is in different quadrants. (c) & (d) Spindle and table coordinate systems respectively with rotation directions .....	96
Figure A3- (a) & (b) Positive rotation of the table for the negative rotation of ‘b’ when the tool vector is in different quadrants. (c) & (d) Spindle and the table coordinate systems respectively with the rotation direction.....	98

# List of table

## *Chapter3*

Table 3.1: Cutting system parameters.....	42
Table 3.2: Minimum cutter length needed at some colloidal cutter locations of 2 <sup>nd</sup> tool path.....	46

## *Chapter4*

Table 4. 1: Machine constant parameters for DMU 60 T.....	58
---	----

# Chapter 1

## Introduction

Five axis machining is the most emerging CNC machining field and widely used technology for the production of complex 3D sculptured surfaces. Examples include, aerospace and automotive parts, and die/mold surfaces. Five axis milling machines are NC machines which are characterized by three translational and two rotary axes. To grab the object in the space at any orientation by the robot, we need minimum five degrees of freedom in the arm of the robot. Similarly, in the CNC machine tools five degrees of freedom are the minimum requirement to achieve any orientation of the tool relative to the work piece.

### 1.1 Classification of 5-Axis machines

Five axis machines can be classified into four groups based on the number of translational and rotary axes [1, 27]:

1. Three translational axes and two rotary axes.
2. Two translational axes and three rotary axes.
3. One translational axis and four rotary axes and
4. Five rotary axes.

A typical five axis machine has three translational axes and two rotary axes. These machine axes can be assigned to the tool and to the machine table using a variety of combinations. Nowadays, five axis machines are commercially available in different variety of location of axis combinations. Five axis machines can be classified on the basis of the location of the two rotary axes as shown in figure 1.1.

1. Table-rotating/tilting: Both rotary axes are carried by the table.
2. Spindle-rotating/tilting: Both rotary axes are carried by the spindle.
3. Table/spindle-tilting: One rotary axis with the table and other one with the spindle.

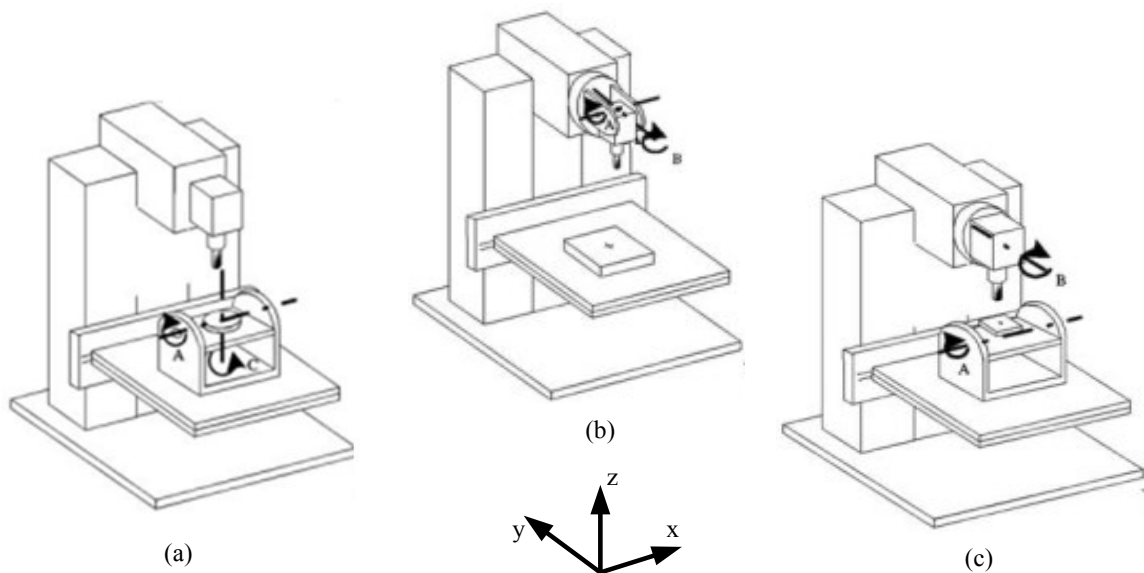


Figure 1.1- Types of 5-axis milling machines: (a) Table-rotating/tilting type (b) Spindle-rotating /tilting type (c) Table/spindle –tilting type

Depending upon the applications, one of the above varieties of the machines can be the suitable for machining the part. For example light and limited dimensions of the work piece are suitable for machining on type 'a' and type 'c' and all types of very heavy and large work pieces such as wings of the air plane, blade of turbines and etc. are suitable for machining on type 'b' machines. The focus of this research is on the machines whose one rotary axis is implemented in the tool kinematic chain and other is on the work piece kinematic chain. These types of machine with different configurations are available in the market. DMU 60T is an example of type 'c' machine whose configuration and some advantages and disadvantages will be addressed in the next section.

### **1.1.1 Configuration of DMU 60T 5-axis machine**

In this machine, two translational axes (x and y) and one rotary axis-b (rotation about y-axis) are implemented with the spindle and one translational Z-axis and one rotary axis-C (rotation about Z-axis) are implemented on the table. Figure 1.2 shows all the axis location with the travel directions.

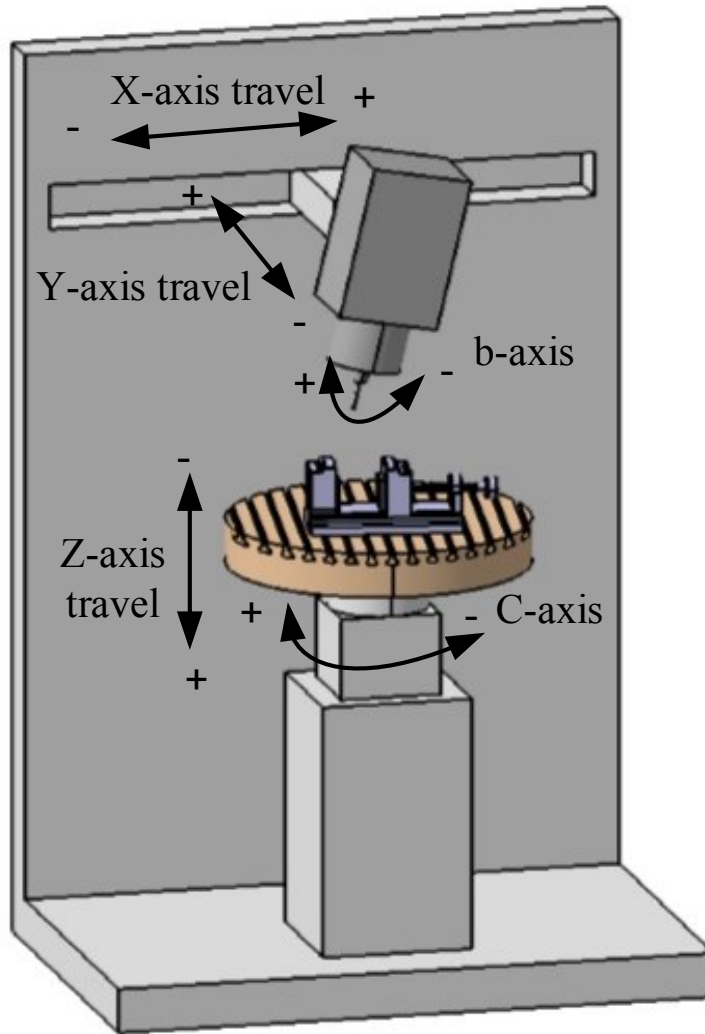


Figure 1.2- Configuration of DMU 60T 5-axis milling machine

### 1.1.2 Advantages and Disadvantages

This type of machine is used for the production of smaller size work piece. Since the table is always horizontal during the machining, gravitational force helps to fix the part on the table. The use full work space is smaller which means space or volume where work piece and tool can shake hand is smaller. The transformation of the work piece coordinates

i.e. tool position ( $CL_x, CL_y, CL_z$ ) and orientation ( $I_x, I_y, I_z$ ) to the machine axes positions i.e. machine translational axes ( $xy$  and  $Z$ ) and rotational axes ( $b$  and  $C$ ) is depends on the position of the work piece on the table. It means, with the change in setup of part on the table, machine axes positions need to be recalculated and a new CNC program must be generated again. Cause of this disadvantage is the location of one rotary axis with the table where work piece is mounted. The 5-axis machines whose both rotary axes are located on the table have the same disadvantage.

To machine the part, two steps of tool path planning and post processing must be accomplished prior to the machining and the following section will describe the details of these two steps.

## **1.2 Tool path generation**

Tool path generation method for the five axes machining normally consists of two steps. In first step cutter contact points are generated on the design surface and in the second step inclination ( $\alpha$ ) and tilt ( $\beta$ ) angles are determined to eliminate gouging. These two steps can be accomplished with the different methodologies and several researchers adopted different methods to complete these steps. List of methods or research topic under these two major issues in the tool path generation of the 5-axis machines are shown in figure 1.3.

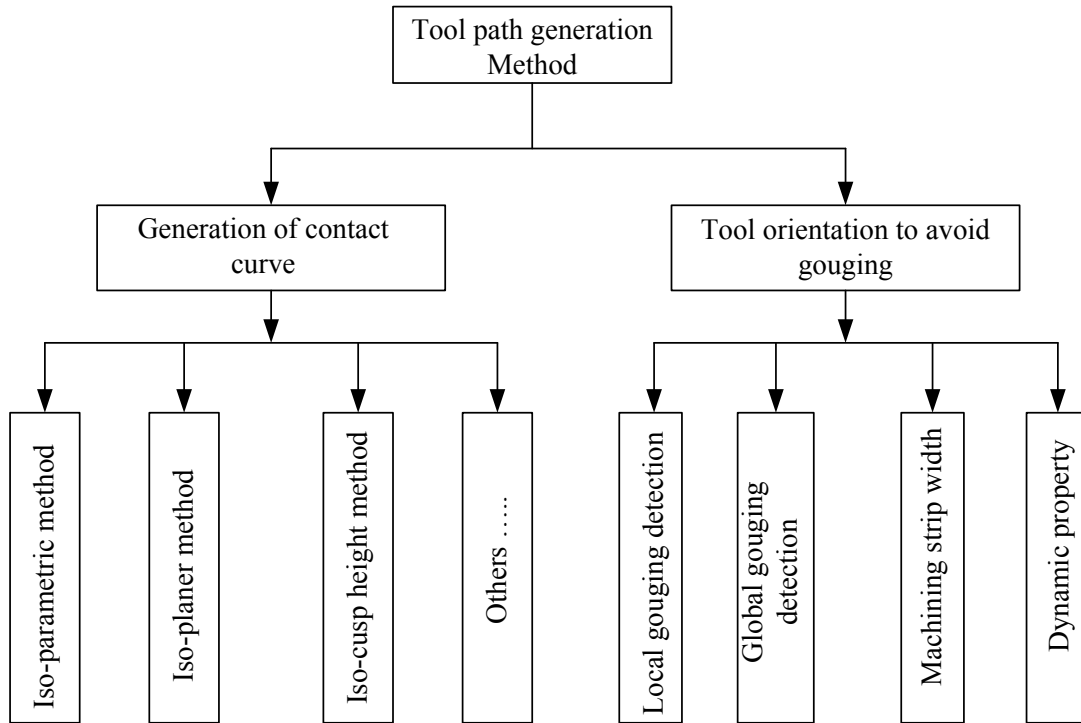


Figure 1.3-Tool path generation method research topics for 5-axis machining

Many existing CAD/CAM software are capable of generating tool path with different machining strategies. CATIA is the most popular CAD/CAM software among them, which allows us to generate five axis machine tool paths with different styles. These tool path styles include;

1. Zigzag tool path
2. One way tool path
3. Out ward helical tool path
4. In ward helical tool path, etc.

CATIA is also providing the opportunity for the user to select the following machining parameters, while using the different functions of the tool path generation.

1. Cutting tool selection i.e. Ball end mill, flat end mill, etc.
2. Selection of no. of level of the machining
3. Machining tolerance selection
4. Scallop height selection
5. Local gouging detection
6. Depth of cut selection
7. Different options for the determination of tool vector i.e. Tool vector normal to the drive surface, optimize lead angle, fixed lead angle, etc.
8. Machining macro selection i.e. tool retract, tool approach, tool linking approach, etc.

By using above options, one can easily generate the five axis tool path (cutter location and orientation) in the part coordinate system. This tool path can be used for any configuration of 5-axis machines. All the research work which is going to be present in this dissertation, is based on the given tool path.

### **1.3 Post processing**

After generating the tool path in the part coordinate system, it is necessary to transform cutter location point ( $CL_x, CL_y, CL_z$ ) and tool orientation vector ( $I_x, I_y, I_z$ ) into machine coordinate system, which are three translations and two rotation angles values depending upon the configuration of the 5-axis machine. These machine coordinates

control the motions of the machine through G-code. Development of G-codes from CL and tool orientation data is called post processing. Series of transformation required for the post processing depends on the machine configuration. This transformation is also called geometry transform or inverse kinematics. Inverse kinematics always gives the multiple solutions and in 5-axis milling machining with two rotary axes, there are four sets of solutions for rotation angles can be possible. For DMU 60T, machine coordinates can be represented in terms of work piece coordinate system as follows

Machine rotations angle;

$$C = f(I_x, I_y)$$

$$b = f(I_z)$$

Machine translational axes;

$$x = f(CL_x, CL_y, I_x, I_y, I_z)$$

$$y = f(CL_x, CL_y, I_x, I_y)$$

$$Z = f(CL_z, I_z)$$

Above equations represents machine axis coordinates in terms of work piece coordinate system and the detailed derivation of the machine coordinates will be presented in the chapter 4 of this dissertation.

## **Chapter 2**

# **Literature Review and Research Objectives**

The research problems, which are not completely defined yet, can be defined simply in two key words sentences

1. Shortest cutter determination without collision.
2. Maximum utilization of the useful work space of the 5-axis machine tools.

Above two research problems are related with the gouging detection and the post processing (G-code development). Therefore, in the following literature review section, first the overview of the existing software capability will be discussed then detailed literature review over the collision & gouging detection and post processing issues in 5-axis machining will be presented.

### **2.1 Literature review**

As mentioned earlier in chapter 1, that in the five axes machining, there is also increase in the possibility of global as well as local collision between the moving parts along with the increase in the flexibility of the tool orientation relative to the work piece. Global collision means accidental contact of non active cutting portion of the cutting system (tool, tool holder and spindle) with the other moving parts of machine such as work

piece or fixture or table. Local collision also refers to as the local gouging, which can occur between the active cutting edge of the tool with the work piece in the vicinity of the cutter contact point.

### **2.1.1 Software overview**

Many existing commercial CAM softwares such as VERICUT, Master cam, and CATIA are capable of detecting collision during the machining simulation. In CATIA, user can adjust tool tilt and inclination angle to get the collision free tool path. Once collision free tool path is generated and G-codes are generated, VERICUT can detect the collision in the actual machining environment. But the collision avoidance task in the actual machining environment is left for the user. After the local collision free tool path generation, it is necessary to check the collision in the actual machining environment and select the optimal tool length which could avoid the global collision. There are two ways to get the optimum cutter length by avoiding collision detection. One is to fix the tool holder design and change the mounting position of the tool in the tool holder. The other is to change the design of the tool holder, to get minimum overhang tool length. In the first case, overall length of the cutting system will increase and in the second case, overall cutting system length will not increase. Also in the second option, less overhang tool length can give low tool slender parameter ' $L^3/D^4$ ', which is the most important parameter in the static tool deflection [2-4].

### 2.1.2 Literature review on collision detection

Most of the algorithms [5-10] used design surface properties such as curvature, in order to get local collision free tool path. Lee [5], first determine the feasible tool orientations for the local surface shape and then avoid rear collision by using the global geometry and updating the feasible tool orientation region. CC. Lo [6] proposed method of cutter path planning in which cutter inclination angle adaptively tune along the machining path in such a way that the effective cutter radius is always maximized, without causing rear gouging. Gray et al. [7, 8] presented a local collision free new positioning strategy of the tool, called RBM (Rolling ball method). Other approach is an arc intersection method (AIM) in which instead of iteratively tilting the tool and checking for the contact with the design surface, the shadow grid points (SGP) of the tool on the surface are rotated to contact the tool. The largest tilt angle is found among the SGP and the tool surface. B.K Choi [9] developed expression for the cusp height as a function of tool orientation angles. Objective of the research was to minimize cusp height with no local and global interference. C.G. Jensen et al. [10] used local distance between the cutter bottom and the surface to detect and avoid the local interference and for the global interference avoidance the shortest distance between the part surface and the cutter axis is calculated.

In the previous research, [11-13] researchers developed the algorithms for rapidly detecting and avoiding the collision based on the hierarchical bounding boxes, called k-discrete oriented poly tope (k-DOP). The work piece modelled as the point cloud data and the tool is modelled with help of implicit equations. Ho et al. [14] developed algorithm for collision detection of the cutting system with the point cloud data. Representation of cutting

system was in constructive solid geometry (CSG) or binary space partition (BSP). Binary space partition determines whether the point into consideration is in collision or not. Illushin et al. [15] used the axial symmetry nature of the cutting system to derive a precise polygon-tool intersection for the global collision detection. Wein et al. [16] extended the approach [15] for the continuous motion of the tool. However both algorithms are effective for global collision detection, not for the removal of collision by the optimum tool length. Lauwers et al. [17] integrated tool path generation module, post processor and machining simulation in order to find global collision and by changing the tool orientation in the tool path generation process, avoidance of collision was possible. The latest technique [37] for the collision detection during the tool path planning of the five axis high speed machining is the image based strategy, which is more efficient and maintain a high detection precision.

Collision detection problems are also addressed for particular applications. Younge et al. [18] proposed algorithm for the collision detection between the cutting tool and the centrifugal impeller blade surface during machining. Gain et al. [19] proposed collision detection algorithm for five axis machining of cavity regions with undercut. This algorithm used the concept of vector field and open region to determine collision free tool orientation. Kim et al. [20] proposed algorithm of the collision detection for five axis machining of a cooling pin which removes the heat from the chips of the computer.

### **2.1.3 Literature review on post processing**

Fully utilization of the five axis NC machines tool working space is an important task. Generally the part size, the cutting system length, the tool orientations and the initial setup of the part on the table determine whether the part could be machined completely without over travel limits of the machine tool or not. Detailed analysis of the kinematics of the different 5-axis machine tools configuration has been presented in [1, 27] along with the some useful definitions of the work space utilization factor, machine tool space efficiency and orientation space index. Several researchers raised the post processing issues such as optimization of the rotations to minimize the kinematic errors near the stationary points of the machined surface [21], minimization of the phase reverse processes and an efficient post processing of the table tilting and rotating 5-axis machines [22, 23], avoiding singularities of 5-axis machine tools [24] and design of generic five axis postprocessor system for different five axis machine tools [25]. Consideration of the setup parameters of the part with respect to the mounting table to utilize the maximum workspace of the machine tools is completely ignored by the researchers [21-25]. To the best of my knowledge only one Journal publication [26] about the optimization of the setup parameters of the 5-axis machine tools to minimize the kinematic errors has been reported yet.

## **2.2 Research problems and objectives**

Based on the literature review conducted in the previous section, research problems are identified and to solve these problems, certain objectives are set.

### **2.2.1 Identification of the research problems**

It is clear that all previous algorithms are able to detect collision for the five axis machining. Most of the algorithms are only capable of the collision detection. Some of them are able to remove collision by changing the tool orientation during the tool path generation. There is no algorithm available which determines the shorter effective cutting edge of the cutting system (tool, tool holder and spindle) of the five axis machine tools based on the predetermined tool path and work in process model. In the industries, different sizes of the tool holders are available and there is no algorithm available for the selection of the tool holder for the five axes machining, which gives the shorter over all cutting system length.

Overall cutting system length is also an important parameter for the determination of the use full work space of the five axis machines. Literature review of the post processing issues also reveals that no research is conducted on the setup parameters of the part to do the complete machining without over travel limits of the machine translational axes. This research problem actually suppress one of the disadvantage of 5-axis machines whose one or two rotary axis are located on the table and mentioned by Bohez et al [1].

“The transformation of the Cartesian CAD/CAM coordinates ( $XYZIJK$ ) of the tool position to the machine axes positions ( $XYZAB$  or  $C$ ) is dependent on the position of the work piece on the machine table. This means that in case the position of the work piece on the table is changed this cannot be modified by translation of the axes system in the NC program. They must be recalculated.”

In fact above disadvantage is due to the location of the one or two rotary axis on the table where work piece is mounted. When the position of the work piece changes on the table, machine translational axis positions are also changed. Consequently, there is the possibility of reaching the end limits of the translational axes. Since the focus of this research is on the machines whose one rotary axis is located with the table and other with the spindle. Hence method developed in this research is implemented on DMU 60T five axis machine. But this method can be implemented on any type of the configuration of the 5-axis machine tools. Based on the above discussion two problems of research are identified as below, and detail architecture of the research problems is shown in figure 2.1

1. Determination of the shortest cutter length based on collision avoidance between the cutting system and work in process model as well as fixture mounted on the table of the 5-axis machine whose one rotary axis belongs to the table and other with the spindle i.e. DMU 60T.
2. Based on the shortest cutter length and the configuration of the 5-axis machine tool, determination of the setup parameters of mounting the largest work piece on the table without violating the machine tool translational axes travel limitations.

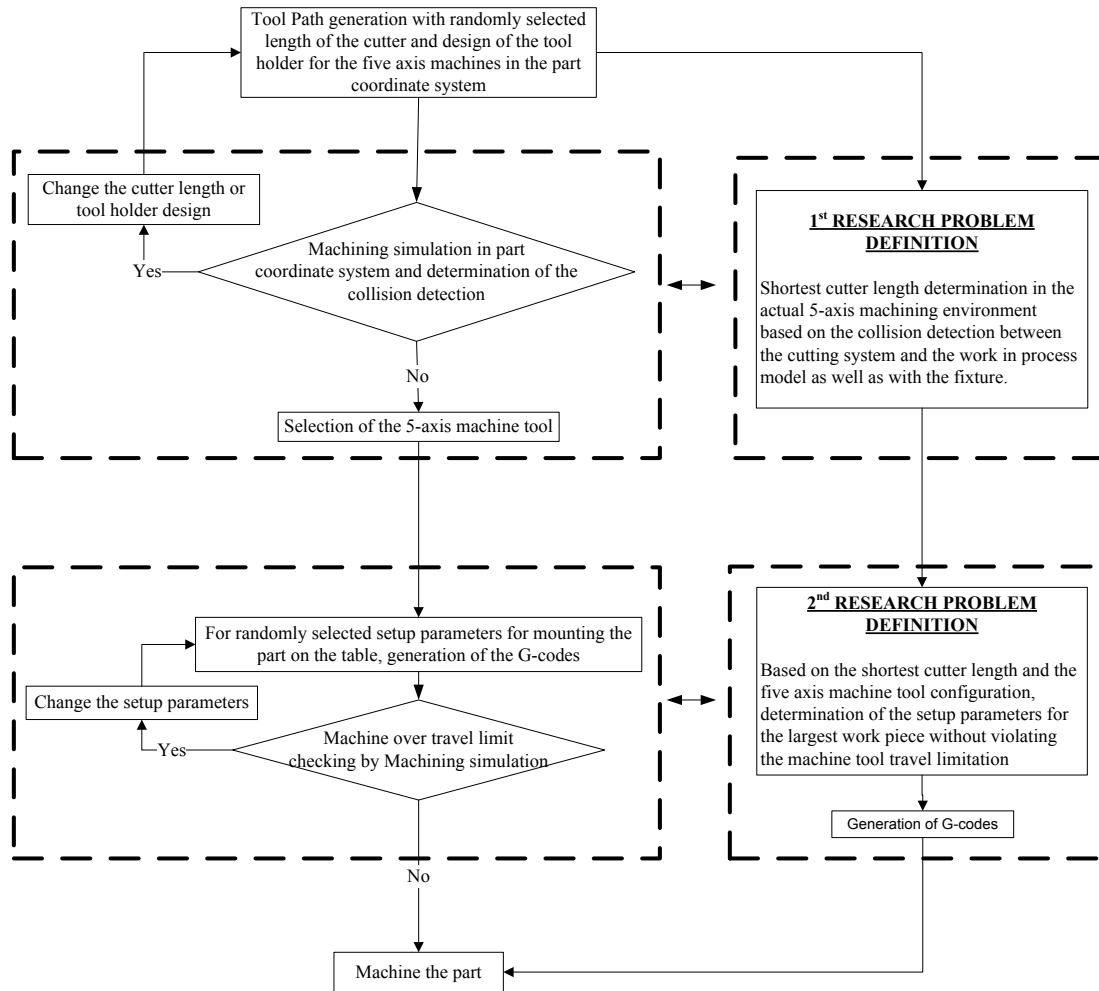


Figure 2.1-Detailed architecture of the research problems definition

## 2.2.2 Research objectives

Based on the above identified 1<sup>st</sup> research problem of shortest cutter length determination, following research objectives are set;

1. Mathematical modelling of the complete cutting system.

2. Development of the mathematical model for the point cloud representation of the work in process model and the fixture
3. Determination of the machine tool rotation angles from the tool vectors in the part coordinate system.
4. Kd-tree data structure employment on the point cloud data for the efficient searching of the colloidal points of the work in process model and the fixture with the complete cutting system.
5. Development of the mathematical model for the interference free cutter length.

Shorter cutter length determines the overall cutting system length and the overall cutting system length determines the tool tip reachable work space for the 5-axis machine. For the maximum utilization of the use full work space based on the shortest cutter length and the setup parameters for mounting the part on the table, following objectives are set;

1. Development of the mathematical model for the determination of the machine tool travel commands of DMU 60T 5-axis machine, when the tool path in the part coordinate system is given.
2. Mathematical model for the determination of the tool tip reachable work space in the table coordinate system.
3. Development of the mathematical model for the determination of the feasible region for the selection of the setup parameters for mounting the work piece on the table.
4. Development of the algorithm for the determination of the feasible region for the selection of the setup parameters for mounting the work piece on the table.

Upcoming two chapters will describe the objectives set in this section. At the end of each chapter, application and practical example of machining the part is also presented along with the verification of the results by simulation.

## Chapter 3

# A Comprehensive Approach to Determining Minimum Cutter Lengths for 5-Axis Milling

The shortest tool determination for the 5-axis milling machining is a critical task. Short tool length increases the rigidity and chatter stability. Besides these advantages, overall short cutting system length can increase the working envelope of the 5-axis machine tools and can minimize the geometrically based error during machining. In this research a new interference detection method of the complete cutting system with the work in process model as well as with the fixture is developed. The complete cutting system includes spindle (cylinder), tool holder (truncated cone) and cutter (cylinder) and is considered as the surface of revolution around the cutter axis. The surfaces of the work-in-process model and the fixture model can be represented as the point cloud data. The KD-tree data structure is employed on point cloud data which gives the efficient searching of the potential candidate points for the interference detection with the complete cutting system.

This chapter comprises of the following five sections. In section 1, possibility of collision in five axis machining is discussed. In section 2, the parametric modelling of the complete cutting system and point cloud data representation of the work in process model or the fixture model is presented. A new interference free cutter length model is presented in section 3. An efficient searching method along with the algorithm is discussed in section 4. The last section concludes the research by discussion of the applications and results.

### 3.1 Types of collision in five axis machining

The collisions that may occur during the machining process depend on the machine type [28]. Focus of this paper is on the “C” type machines collisions detection and removal by the optimum length. The configuration of the machine along with the axes motion is shown in figure 1.2. It is obvious from the configuration of the machine; there is a possibility of the cutting system collision with the in-process work piece or the fixture model. The cutting system includes the spindle, the tool holder and the tool. Illustration of the spindle collision with the fixture model is shown in figure 3.1.

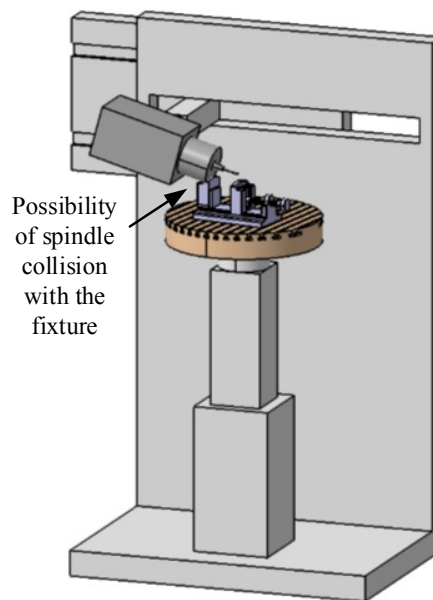


Figure 3.1- Possibility of the spindle collision with the fixture in actual machining environment

### 3.2 Cutting system model and point cloud representation of the in-process or the fixture model

Three bodies which include the complete cutting system, the in-process work piece

model and the fixture model are the possible candidates of the collision during the machining. Due to the axial symmetry nature of the cutting system, the spindle is represented as a cylinder and the tool holder as a truncated cone.

### 3.2.1 Parametric CAD model of the cutting system

Cutting system can be represented in the cutter coordinate system as a surface of revolution. Figure 3.2 shows the planer lines along with the end points. These planer lines are used to generate surface of revolution.

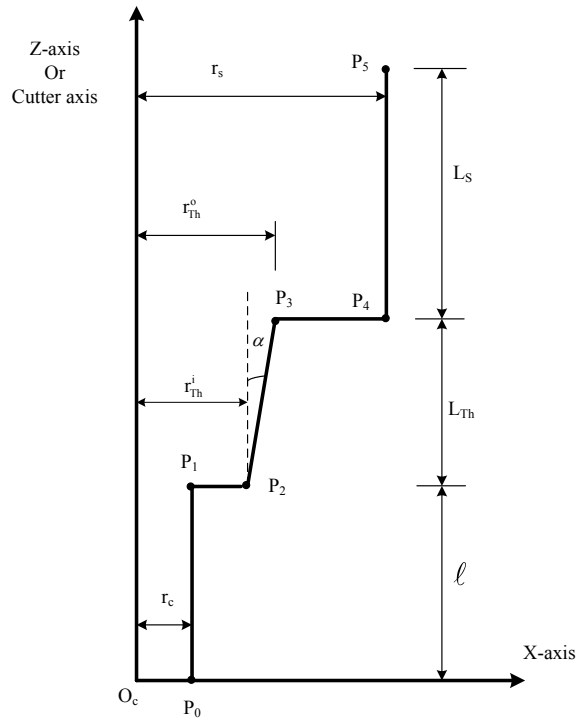


Figure 3.2- Cutting system profile in the cutter coordinate system

The parametric form of the line segments can be given as;

$$L_n(u) = (1-u) \cdot P_{n-1} + u \cdot P_n \quad (0 \leq u \leq 1) \quad \text{for } n=1,2,\dots,5 \quad (3.1)$$

The surface of revolution can be obtained by inserting another parameter ( $\varphi$ ). Therefore,

$$S_n(u, \varphi) = R_z(\varphi) \cdot L_n(u) \quad \begin{pmatrix} 0 \leq u \leq 1 \\ 0 \leq \varphi \leq 2\pi \end{pmatrix} \quad \text{for } n=1,2,\dots,5 \quad (3.2)$$

$$\text{Where, } R_z(\varphi) = \begin{bmatrix} \cos(\varphi) & -\sin(\varphi) & 0 \\ \sin(\varphi) & \cos(\varphi) & 0 \\ 0 & 0 & 1 \end{bmatrix} \quad 0 \leq \varphi \leq 2\pi$$

### 3.2.2 In-process work piece model

Different CAM softwares are able to generate tool paths and also capable to store the updated stock after each cutting process. These updated stocks are called in-process work piece models. For an illustration, a rough tool path is generated in CATIA and from STL file of the in-process work piece model, a tessellated triangular mesh surface is generated. Demonstration of the work in process model is shown in figure-3.3 and the tessellated triangular representation of the in-process work piece model is shown in figure-3.4.

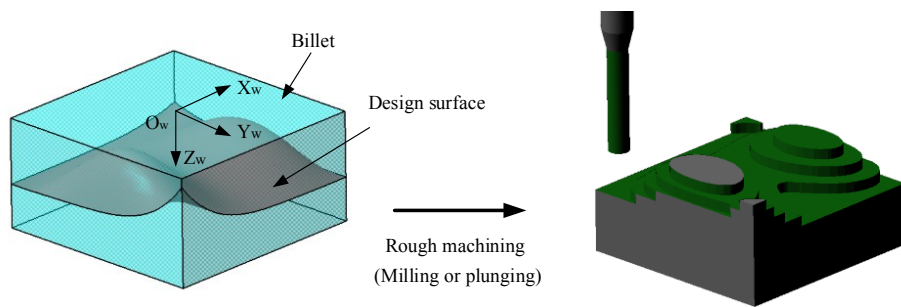


Figure 3.3- In process work piece model after roughing operation

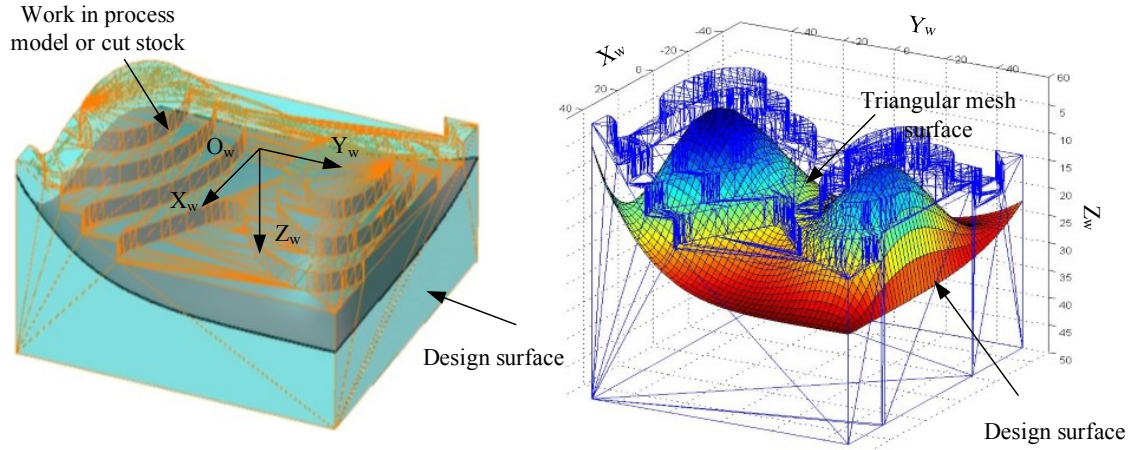


Figure 3.4- Tessellated triangular representation of the in-process work piece model

### 3.2.3 Point cloud generation

Randomize points generation with the suitable density (points per unit area) will create point cloud data. In the triangular tessellation representation of the in-process work piece model, point cloud data consist of the vertices of the triangles and randomly generated points on the triangular planes with the suitable density. The method of generating random points on a triangle is well established. For generating the point cloud data of constant density “D” for each triangle, no. of points on each triangle can be calculated as

$$\text{No. of points for a triangle} = \frac{1}{2} \cdot \left| \overline{P_1P_2} \times \overline{P_1P_3} \right| \cdot D \quad (3.3)$$

Where  $P_1$ ,  $P_2$  and  $P_3$  are the vertices of a triangle

For the generation of a random point on a triangle, two random numbers  $r_1$  and  $r_2$  at the interval of  $[0, 1]$  are generated and point can be calculated by the following formula as given in the literature [29, 30]

$$P = (1 - \sqrt{r_1}) \cdot P_1 + \sqrt{r_1} \cdot (1 - r_2) \cdot P_2 + \sqrt{r_1} \cdot r_2 \cdot P_3 \quad (3.4)$$

Example of the point cloud data generation with the density of  $0.5 \text{ points/mm}^2$  on the triangular mesh surface is shown in figure 3.5. No. of points and points on the triangles are calculated by using equations (3.3) and (3.4) respectively.

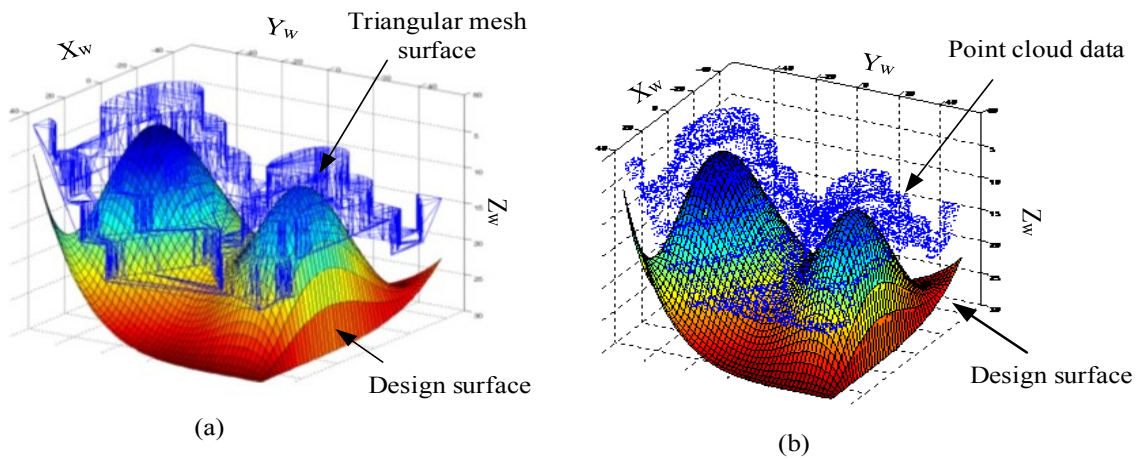


Figure 3.5- (a) Triangular mesh surface (b) point cloud data with  $D=0.5 \text{ points/mm}^2$

### 3.3 The interference free cutter length model

First at the initial clamping position of the tool, tool length( $l$ ) is assumed as an initial tool length. Based on this tool length, the spindle interference free cutter length model is established and a new spindle interference free tool length is calculated. Then

based on a new tool length( $l_{new}$ ), the tool holder interference free cutter length model is established and the final interference free cutter length is determined.

### 3.3.1 Spindle interference free cutter length model

Objective function can be formulated as to find the minimum distance  $d(u)$  between the sample point (point cloud data) on the work in process model as well as on the fixture and the tool center line segments from the spindle start point to the pivot point.

Condition for the avoidance of collision is given as;

Minimum distance  $[d(u)] > r_s(u)$  (radius of the spindle)

$$L_s(u) = (1-u) \cdot P_w^{SS} + (u) \cdot P_w^{SE} \quad \left( \begin{array}{l} 0 \leq u \leq 1 \\ L_s(u) \in \text{Tool vector} \end{array} \right) \quad (3.5)$$

$$\begin{bmatrix} P_w^{SS} & P_w^{SE} \end{bmatrix} = T_w^C \cdot \begin{bmatrix} P_C^{SS} & P_C^{SE} \end{bmatrix} \quad (3.6)$$

Where,

$P_C^{SS} = [0 \ 0 \ l + L_{Th} \ 1]^T$  = Spindle center line start point in the cutter coordinate system

$P_C^{SE} = [0 \ 0 \ l + L_{Th} + L_s \ 1]^T$  = Spindle center line end point in the cutter coordinate system

$$T_w^C = \begin{bmatrix} \cos(b) \cdot \sin(C) & \cos(C) & \sin(b) \cdot \sin(C) & CL_x \\ \cos(b) \cdot \cos(C) & -\sin(C) & \sin(b) \cdot \cos(C) & CL_y \\ \sin(b) & 0 & -\cos(b) & CL_z \\ 0 & 0 & 0 & 1 \end{bmatrix}$$

Where  $T_w^C$  is the homogeneous transformation matrix from the cutter coordinate system to the work piece coordinate system and C and b are the machine tool rotations

determined by the tool vectors  $[I_x I_y I_z]$  (For details of derivation see Appendix A). And  $[CL_x CL_y CL_z]$  are the cutter locations in the part coordinate system.

The minimum distance can be calculated as

$$d(u) = \sqrt{(x_{SP} - x(u))^2 + (y_{SP} - y(u))^2 + (z_{SP} - z(u))^2} \quad (3.7)$$

Where,

$$[x_{SP} \ y_{SP} \ z_{SP}]^T \in \text{Point cloud data}$$

$$[x(u) \ y(u) \ z(u)]^T \in L_s(u)$$

The parameter at which  $[x(u) \ y(u) \ z(u)]^T$  is calculated, can be find as

$$u = \frac{(x_{SP} - x_w^{SS}) \cdot (x_w^{SE} - x_w^{SS}) + (y_{SP} - y_w^{SS}) \cdot (y_w^{SE} - y_w^{SS}) + (z_{SP} - z_w^{SS}) \cdot (z_w^{SE} - z_w^{SS})}{L_s^2} \quad (3.8)$$

### 3.3.2 Tool holder interference free cutter length model

Objective function can be formulated as to find the minimum distance  $d(u)$  between the sample point (point cloud data) on the work in process model as well as on the fixture and the tool center line segments from the tool holder start point to the tool holder end point. Condition for the avoidance of collision is given as;

Minimum distance  $[d(u)] > r_{Th}(u)$  (radius of the tool holder)

$$r_{Th}(u) = r_{Th}^i + (r_{Th}^o - r_{Th}^i) \cdot u \quad (3.9)$$

$$L_{Th}(u) = (1-u) \cdot P_w^{ThS} + (u) \cdot P_w^{ThE} \quad \left( \begin{array}{l} 0 \leq u \leq 1 \\ L_{Th}(u) \in \text{Tool vector} \end{array} \right) \quad (3.10)$$

$$\begin{bmatrix} P_w^{ThS} & P_w^{ThE} \end{bmatrix} = T_w^C \cdot \begin{bmatrix} P_C^{ThS} & P_C^{ThE} \end{bmatrix} \quad (3.11)$$

Where,

$r_{Th}^o$  = Larger radius of the tool holder (truncated cone)

$r_{Th}^i$  = Smaller radius of the tool holder

$P_C^{ThS} = [0 \ 0 \ l_{new} \ 1]^T$  = Tool holder start point in the cutter coordinate system.

$P_C^{ThE} = [0 \ 0 \ l_{new} + L_{Th} \ 1]^T$  = Tool holder end point in the cutter coordinate system.

Minimum distance can be calculated as

$$d(u) = \sqrt{(x_{SP} - x(u))^2 + (y_{SP} - y(u))^2 + (z_{SP} - z(u))^2} \quad (3.12)$$

$[x_{SP} \ y_{SP} \ z_{SP}]^T \in \text{Point cloud data}$

$[x(u) \ y(u) \ z(u)]^T \in L_{Th}(u)$

The parameter at which  $[x(u) \ y(u) \ z(u)]^T$  is calculated, can be find as

$$u = \frac{(x_{SP} - x_w^{ThS}) \cdot (x_w^{ThE} - x_w^{ThS}) + (y_{SP} - y_w^{ThS}) \cdot (y_w^{ThE} - y_w^{ThS}) + (z_{SP} - z_w^{ThS}) \cdot (z_w^{ThE} - z_w^{ThS})}{(L_{Th})^2} \quad (3.13)$$

### **3.4 The new search method for minimum cutter lengths**

The model presented in section 3.3 is not the efficient way of finding the optimum tool length. It is necessary to confine the searching of the colloidal points in the local region instead of searching the whole point cloud data. In order to get the local region for searching the colloidal points at each cutter location, Kd-tree data structure is employed on the point cloud data. The multidimensional binary tree (Kd-tree) was first described by Bentley [31]. In the Kd-tree data structure no bisector is required as in the two dimensions quad-tree data structure [32]. Therefore, Kd-tree data structure has superior performance in contrast with the quad-tree data structure for the range searching queries [33]. For collision detection queries in 5-axis machining, previous researcher [23, 28] used octree bounding box volume hierarchical tree structure to represent the colloidal parts. In this research, orthogonal range searching queries from Kd-tree data structure is implemented for the collision detection.

#### **3.4.1 Two dimension Kd-tree data structure**

Two dimension Kd-tree data structure for the point cloud data can be built by taking the projection of the 3D points onto the xy-plane ( $z=0$ ). A brief illustration of two dimension Kd-tree data structure along with the orthogonal range searching query is presented here. Let  $P_i$  be the set of points for  $i=1, 2, \dots, 10$  in two dimension  $(x_i, y_i)$ . The idea is to first split the points into two halves based on x-coordinate, then on y-coordinate, then again on x-coordinate, and so on in alternating fashion. This process of splitting up of two dimension regions is continued until the size of the subset values store in sub tree reaches

a minimum value “c”. Figure 3.6(a) and 3.6(b) shows the bisecting lines and the Kd-tree data structure respectively for  $c=1$ .

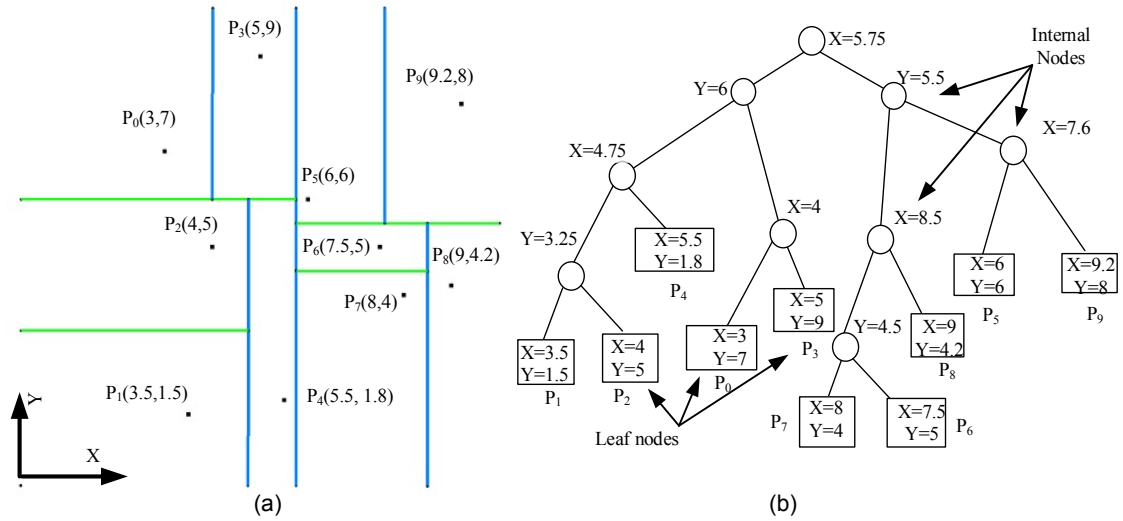


Figure 3.6- (a) Bisecting of the data points (b) Kd-tree data structure

After constructing the Kd-tree data structure several queries such as to find the exact matching of a point, to find the nearest neighbour of a point or to find the points which are in the given orthogonal range can be addressed efficiently. Since the focus of this research is on the orthogonal range searching queries, hence in figure 3.7 it can be seen that how to find the points for the given orthogonal range  $[x_{\min} = 7 \quad x_{\max} = 10 \quad y_{\min} = 7.5 \quad y_{\max} = 10]$ .

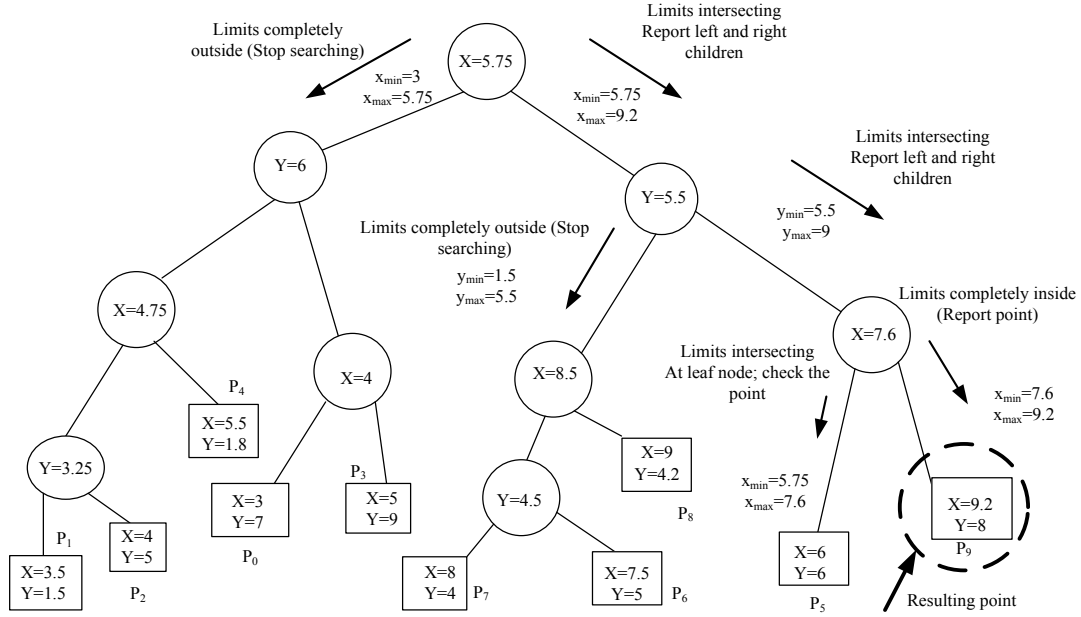


Figure 3.7- Checking procedure for the orthogonal searching query

### 3.4.2 Orthogonal range determination model for the spindle

The orthogonal range of the spindle body in x and y directions of the work piece coordinate system can be determined by the projections of the top and the bottom circle of the spindle on xy-plane of the work piece coordinate system. Equation of the bottom circle of the spindle ‘(BC)<sub>s</sub>’ in the work-piece coordinate system can be represented as

$$\begin{bmatrix} x_w(\theta) \\ y_w(\theta) \\ z_w(\theta) \\ 1 \end{bmatrix} = \begin{bmatrix} \sin(C) \cdot \cos(b) & \cos(C) & \sin(C) \cdot \sin(b) & CL_x \\ \cos(C) \cdot \cos(b) & -\sin(C) & \sin(b) \cdot \cos(C) & CL_y \\ \sin(b) & 0 & -\cos(b) & CL_z \\ 0 & 0 & 0 & 1 \end{bmatrix} \cdot \begin{bmatrix} r_s \cdot \cos(\theta) \\ r_s \cdot \sin(\theta) \\ l + L_{Th} \\ 1 \end{bmatrix}$$

Elliptical projection of the spindle bottom circle on  $x_w y_w$ -plane i-e  $z_w(\theta) = 0$  is given by

$$\begin{bmatrix} x_w(\theta) \\ y_w(\theta) \end{bmatrix} = \begin{bmatrix} r_s \cdot \cos(\theta) \cdot \sin(C) \cdot \cos(b) + r_s \cdot \sin(\theta) \cdot \cos(C) \\ r_s \cdot \cos(\theta) \cdot \cos(C) \cdot \cos(b) - r_s \cdot \sin(\theta) \cdot \sin(C) \\ + \sin(C) \cdot \sin(b) \cdot (l + L_{Th}) + CL_x \\ + \sin(b) \cdot \cos(C) \cdot (l + L_{Th}) + CL_y \end{bmatrix} \quad (3.14)$$

In order to find the minimum value of  $x_w$  and  $y_w$ , differentiate  $x_w(\theta)$  and  $y_w(\theta)$  with respect to  $\theta$  and set it equal to zero i.e.  $\frac{dx_w(\theta)}{d\theta} = 0$  and  $\frac{dy_w(\theta)}{d\theta} = 0$

After differentiation and simplification, we get

$$\theta_{x(\min)} = \arctan\left(\frac{\cos(C)}{\sin(C) \cdot \cos(b)}\right) \quad (3.15)$$

Similarly value of  $\theta_{y(\min)}$  can be calculated as

$$\theta_{y(\min)} = \arctan\left(\frac{-\sin(C)}{\cos(C) \cdot \cos(b)}\right) \quad (3.16)$$

The minimum values of  $x_w$  and  $y_w$  can be found by replacing  $\theta = \theta_{x(\min)}$  and  $\theta = \theta_{y(\min)}$  in equation (3.14).

$$\begin{bmatrix} \text{Min}(x_w) \\ \text{Min}(y_w) \end{bmatrix}_{(BC)_s} = \begin{bmatrix} r_s \cdot \cos(\theta_{x(\min)}) \cdot \sin(C) \cdot \cos(b) + r_s \cdot \sin(\theta_{x(\min)}) \cdot \cos(C) \\ r_s \cdot \cos(\theta_{y(\min)}) \cdot \cos(C) \cdot \cos(b) - r_s \cdot \sin(\theta_{y(\min)}) \cdot \sin(C) \\ + \sin(C) \cdot \sin(b) \cdot (l + L_{Th}) + CL_x \\ + \sin(b) \cdot \cos(C) \cdot (l + L_{Th}) + CL_y \end{bmatrix}$$

To calculate the maximum values of  $x_w$  and  $y_w$ , first coordinates of the center of the elliptical projection of the spindle bottom circle ‘ $(CBC)_s$ ’ in the work piece coordinate system is calculated and it is given by

$$\begin{bmatrix} x_w \\ y_w \end{bmatrix}_{(CBC)_s} = \begin{bmatrix} \sin(C) \cdot \sin(b) \cdot (l + L_{Th}) + CL_x \\ \sin(b) \cdot \cos(C) \cdot (l + L_{Th}) + CL_y \end{bmatrix}$$

The maximum values of  $x_w$  and  $y_w$  coordinates of the spindle bottom circle ‘(BC)<sub>s</sub>’ in the work piece coordinate system can be calculated with the help of the center of the ellipse as follows

$$\begin{bmatrix} \text{Max}(x_w) \\ \text{Max}(y_w) \end{bmatrix}_{(BC)_s} = \begin{bmatrix} 2 \cdot (x_w)_{(CBC)_s} - \text{Min}(x_w)_{(BC)_s} \\ 2 \cdot (y_w)_{(CBC)_s} - \text{Min}(y_w)_{(BC)_s} \end{bmatrix}$$

Similarly for the top circle of the spindle ‘(TC)<sub>s</sub>’, set of the maximum and the minimum values of  $x_w$  and  $y_w$  coordinates can be determined. For the orthogonal range values of spindle ‘(R)<sub>s</sub>’

$$\begin{bmatrix} \text{Min}(x_w) \\ \text{Max}(x_w) \\ \text{Min}(y_w) \\ \text{Max}(y_w) \end{bmatrix}_{(R)_s} = \begin{bmatrix} \text{Min} \left\{ (\text{Min}(x_w), \text{Max}(x_w))_{(BC)_s} \quad (\text{Min}(x_w), \text{Max}(x_w))_{(TC)_s} \right\} \\ \text{Max} \left\{ (\text{Min}(x_w), \text{Max}(x_w))_{(BC)_s} \quad (\text{Min}(x_w), \text{Max}(x_w))_{(TC)_s} \right\} \\ \text{Min} \left\{ (\text{Min}(y_w), \text{Max}(y_w))_{(BC)_s} \quad (\text{Min}(y_w), \text{Max}(y_w))_{(TC)_s} \right\} \\ \text{Max} \left\{ (\text{Min}(y_w), \text{Max}(y_w))_{(BC)_s} \quad (\text{Min}(y_w), \text{Max}(y_w))_{(TC)_s} \right\} \end{bmatrix} \quad (3.17)$$

### 3.4.3 Algorithm of the collision detection with the spindle (cylinder) and removal by the optimum tool length

Inputs {Work piece coordinates ( $CL_x, CL_y, CL_z, I_x, I_y, I_z$ ), Machine tool rotations ( $b$  &  $C$ ), Length of the tool at initial mounting position ( $l$ ), Spindle length ( $L_s$ ), Tool holder length ( $L_{Th}$ ), Spindle radius ( $r_s$ ), Point cloud data of the work-in-process and the fixture models}

**Step 1:**

At each cutter location, calculate the orthogonal range for the spindle by using equation (3.17) and extract only those points by Kd-tree data structure approach, which have the possibility of the collision.

**Step 2:**

For the given tool vectors or machine tool rotations, cutter locations and the length of the tool at any assumed tool mounting position ( $l$ ). Calculate the start and the end (pivot) points of the spindle center line segments in the work piece coordinate system by using equation (3.6)

**Step 3:**

At each cutter location, calculate the parameters 'u' on the cutting system center line, which give the perpendicular distances from the sample points by using equation (3.8). For the calculations, only use those sample points which are extracted in step 1.

**Step 4:**

If  $0 \leq u \leq 1$  then keep the parameter value as well as corresponding sample point, otherwise neglect it. It is not necessary that all the sample points have perpendicular interaction with the spindle center line segment.

**Step 5:**

Calculate the points on the spindle line segment by using equation (3.5) and distances (d) between these points and corresponding sample points by equation (3.7). Subtract the radius of the spindle from each distance (d) to get  $\Delta d$ ;  $\Delta d = d - r_s$

**Step 6:**

Sort the values of  $\Delta d$  and only consider the negative values, which show the collision with the spindle surface. Also corresponding parametric value “u” is stored.

**Step 7:**

Parametric value ( $0 \leq u \leq 1$ ), can be converted into the actual parameter of the length of the spindle by multiplying “ $L_S$ ”. Also sort out the maximum value of the parameter for each cutter location.

**Step 8:**

If the negative values of the distance in step 6 exist, then we need to increase the length of the tool to avoid collision and the minimum increase in length is the maximum of the maximum values of parameter for each cutter location calculated in step 7. If no negative value of distance  $\Delta d$  is exist, there is no need to increase the length and  $l_{new} = l$

Flow chart of the above algorithm is shown in figure 3.8. At the end of the flow chart, it is indicated that run the algorithm for the collision detection with the tool holder with the spindle collision free length of ( $l_{new}$ ) .

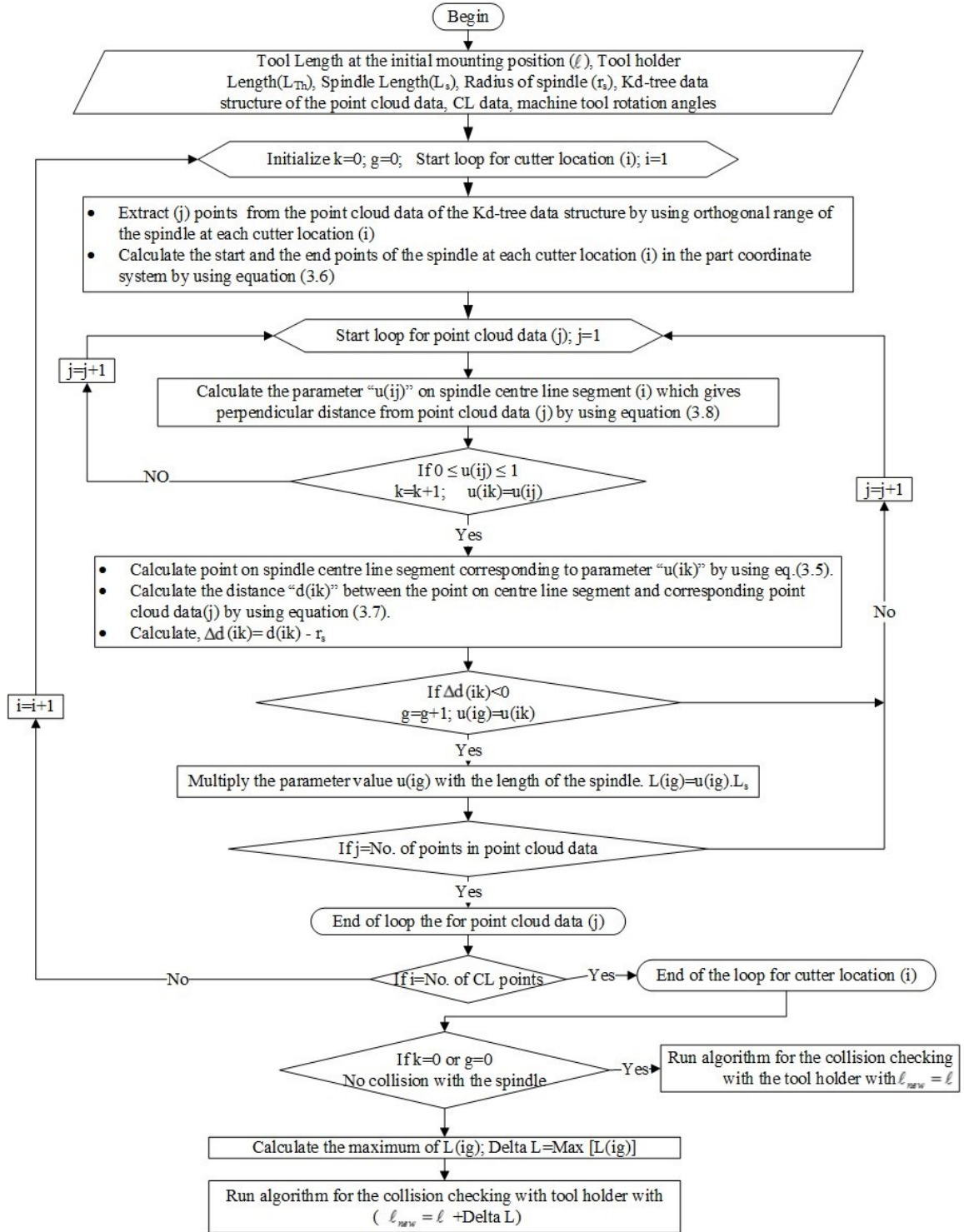


Figure 3.8- Flow chart of the algorithm for the spindle collision detection and removal by the optimum cutter length

Objective of the above algorithm is to get the optimum tool length( $l_{new}$ ), which could avoid the spindle collision with the point cloud data. Based on a new tool length( $l_{new}$ ), orthogonal range searching model for the tool holder can be established.

#### 3.4.4 Orthogonal range determination model for the tool holder

The orientation of the cutter does not change, therefore  $\theta_{x(\min)}$  and  $\theta_{y(\min)}$  can be calculated from equations (3.15) and (3.16) respectively. The minimum and the maximum values of  $x_w$  and  $y_w$  for the bottom and the top circle of the tool holder (truncated cone) can be obtained from the following equations.

***For the bottom circle of the tool holder:***

The minimum values of  $x_w$  and  $y_w$  coordinates for the tool holder bottom circle (BC)<sub>Th</sub> can be given as

$$\begin{aligned} \begin{bmatrix} \text{Min}(x_w) \\ \text{Min}(y_w) \end{bmatrix}_{(BC)_{Th}} &= \begin{bmatrix} r_{Th}^i \cdot \cos(\theta_{x(\min)}) \cdot \sin(C) \cdot \cos(b) + r_{Th}^i \cdot \sin(\theta_{x(\min)}) \cdot \cos(C) \\ r_{Th}^i \cdot \cos(\theta_{y(\min)}) \cdot \cos(C) \cdot \cos(b) - r_{Th}^i \cdot \sin(\theta_{y(\min)}) \cdot \sin(C) \\ + \sin(C) \cdot \sin(b) \cdot (l_{new}) + CL_x \\ + \sin(b) \cdot \cos(C) \cdot (l_{new}) + CL_y \end{bmatrix} \end{aligned}$$

The coordinates of the center of the bottom circle of the tool holder ‘(CBC)<sub>Th</sub>’ is calculated as

$$\begin{bmatrix} x_w \\ y_w \end{bmatrix}_{(CBC)_{Th}} = \begin{bmatrix} \sin(C) \cdot \sin(b) \cdot (l_{new}) + CL_x \\ \sin(b) \cdot \cos(C) \cdot (l_{new}) + CL_y \end{bmatrix}$$

The maximum values of  $x_w$  and  $y_w$  coordinates for the tool holder bottom circle can be given as

$$\begin{bmatrix} \text{Max}(x_w) \\ \text{Max}(y_w) \end{bmatrix}_{(BC)_{Th}} = \begin{bmatrix} 2 \cdot (x_w)_{(CBC)_{Th}} - \text{Min}(x_w)_{(BC)_{Th}} \\ 2 \cdot (y_w)_{(CBC)_{Th}} - \text{Min}(y_w)_{(BC)_{Th}} \end{bmatrix}$$

***For the top circle of the tool holder:***

The minimum values of  $x_w$  and  $y_w$  coordinates for the tool holder top circle  $(TC)_{Th}$  can be given as

$$\begin{bmatrix} \text{Min}(x_w) \\ \text{Min}(y_w) \end{bmatrix}_{(TC)_{Th}} = \begin{bmatrix} r_{Th}^o \cdot \cos(\theta_{x(\min)}) \cdot \sin(C) \cdot \cos(b) + r_{Th}^o \cdot \sin(\theta_{x(\min)}) \cdot \cos(C) \\ r_{Th}^o \cdot \cos(\theta_{y(\min)}) \cdot \cos(C) \cdot \cos(b) - r_{Th}^o \cdot \sin(\theta_{y(\min)}) \cdot \sin(C) \\ + \sin(C) \cdot \sin(b) \cdot (l_{new} + L_{Th}) + CL_x \\ + \sin(b) \cdot \cos(C) \cdot (l_{new} + L_{Th}) + CL_y \end{bmatrix}$$

The coordinates of the center of the top circle of the tool holder ‘ $(CTC)_{Th}$ ’ can be calculated as

$$\begin{bmatrix} x_w \\ y_w \end{bmatrix}_{(CTC)_{Th}} = \begin{bmatrix} \sin(C) \cdot \sin(b) \cdot (l_{new} + L_{Th}) + CL_x \\ \sin(b) \cdot \cos(C) \cdot (l_{new} + L_{Th}) + CL_y \end{bmatrix}$$

The maximum values of  $x_w$  and  $y_w$  coordinates for the tool holder top circle can be given as

$$\begin{bmatrix} \text{Max}(x_w) \\ \text{Max}(y_w) \end{bmatrix}_{(TC)_{Th}} = \begin{bmatrix} 2 \cdot (x_w)_{(CTC)_{Th}} - \text{Min}(x_w)_{(TC)_{Th}} \\ 2 \cdot (y_w)_{(CTC)_{Th}} - \text{Min}(y_w)_{(TC)_{Th}} \end{bmatrix}$$

The tool holder orthogonal range values can be calculated by the following equation

$$\begin{bmatrix} \text{Min}(x_w) \\ \text{Max}(x_w) \\ \text{Min}(y_w) \\ \text{Max}(y_w) \end{bmatrix}_{(R)_{Th}} = \begin{bmatrix} \text{Min} \left\{ (\text{Min}(x_w), \text{Max}(x_w))_{(BC)_{Th}} \quad (\text{Min}(x_w), \text{Max}(x_w))_{(TC)_{Th}} \right\} \\ \text{Max} \left\{ (\text{Min}(x_w), \text{Max}(x_w))_{(BC)_{Th}} \quad (\text{Min}(x_w), \text{Max}(x_w))_{(TC)_{Th}} \right\} \\ \text{Min} \left\{ (\text{Min}(y_w), \text{Max}(y_w))_{(BC)_{Th}} \quad (\text{Min}(y_w), \text{Max}(y_w))_{(TC)_{Th}} \right\} \\ \text{Max} \left\{ (\text{Min}(y_w), \text{Max}(y_w))_{(BC)_{Th}} \quad (\text{Min}(y_w), \text{Max}(y_w))_{(TC)_{Th}} \right\} \end{bmatrix} \quad (3.18)$$

### 3.4.5 Algorithm of the collision detection with the tool holder (truncated cone) and removal by the optimum tool length

Inputs {Work piece coordinates ( $CL_x, CL_y, CL_z, I_x, I_y, I_z$ ), Machine tool rotations (b & C),

New length of the tool after collision removal with the spindle ( $l_{new}$ ), Length of the tool holder ( $L_{Th}$ ), Bottom radius of the tool holder ( $r_{Th}^i$ ), Top radius of the tool holder ( $r_{Th}^o$ ), KD-tree data structure of the point cloud data of the work-in-process model and the fixture model}

#### Step 1:

At each cutter location, calculate the orthogonal range for the tool holder by using equation (3.18) and extract only those points by the Kd-tree data structure approach, which have the possibility of the collision.

#### Step 2:

For the given tool vectors or machine tool rotations, cutter locations and with the new tool length  $l_{new}$ , calculate the start and the end points of tool holder center line segment in work piece coordinate system by using equation (3.11).

**Step 3:**

At each cutter location, calculate the parameters 'u' on the cutting system center line, which give the perpendicular distances from the sample points by using equation (3.13). For the calculations, only use those sample points which are extracted in step 1.

**Step 4:**

If  $0 \leq u \leq 1$  then keep the parameter value as well as corresponding sample point, otherwise neglect it. It is not necessary that all sample points have perpendicular interaction with the tool holder center line segment.

**Step 5:**

Calculate the points on the tool holder center line segment at the valid parametric values of 'u' by using equation (3.10) and also calculate the distances 'd' between the calculated points and the corresponding sample points by using equation (3.12).

**Step 6:**

Calculate the radii 'r' of circles for tool holder at valid parametric value by using equation (3.9).

**Step 7:**

Subtract the radius (r) calculated in step (6) from the distance (d) calculated in step (5) at the corresponding value of the parameter (u). If the resulting value is negative, it means collision. Save the colloidal points and the corresponding parameters (u).

**Step 8:**

By using the distance ( $d$ ) of the colloidal points as the radius of the tool holder ( $r_{Th}$ ), calculate the new value of the parameter ( $u$ ) by using equation (3.9). If the value of the parameter ( $u$ ) is positive, subtract this parameter ( $u$ ) value from the older one stored in step 7 and if the value of the parameter ( $u$ ) is negative or zero, value stored in step 7 will be used.

**Step 9:**

In order to get the actual length of the tool needed to increase for the avoidance of collision for each cutter location, multiply the parametric value of ( $u$ ) calculated in step 8 by the tool holder length ( $L_{Th}$ ) for each colloidal point. The maximum value can be used as increase in the tool length for each cutter location.

**Step 10:**

Maximum of the maximum values of increase in length for each cutter location will be used for the whole tool path.

Flow chart of the above algorithm is shown in figure 3.9. From this algorithm, the final optimum cutter length can be calculated, which can avoid the collision with the spindle as well as with the tool holder.

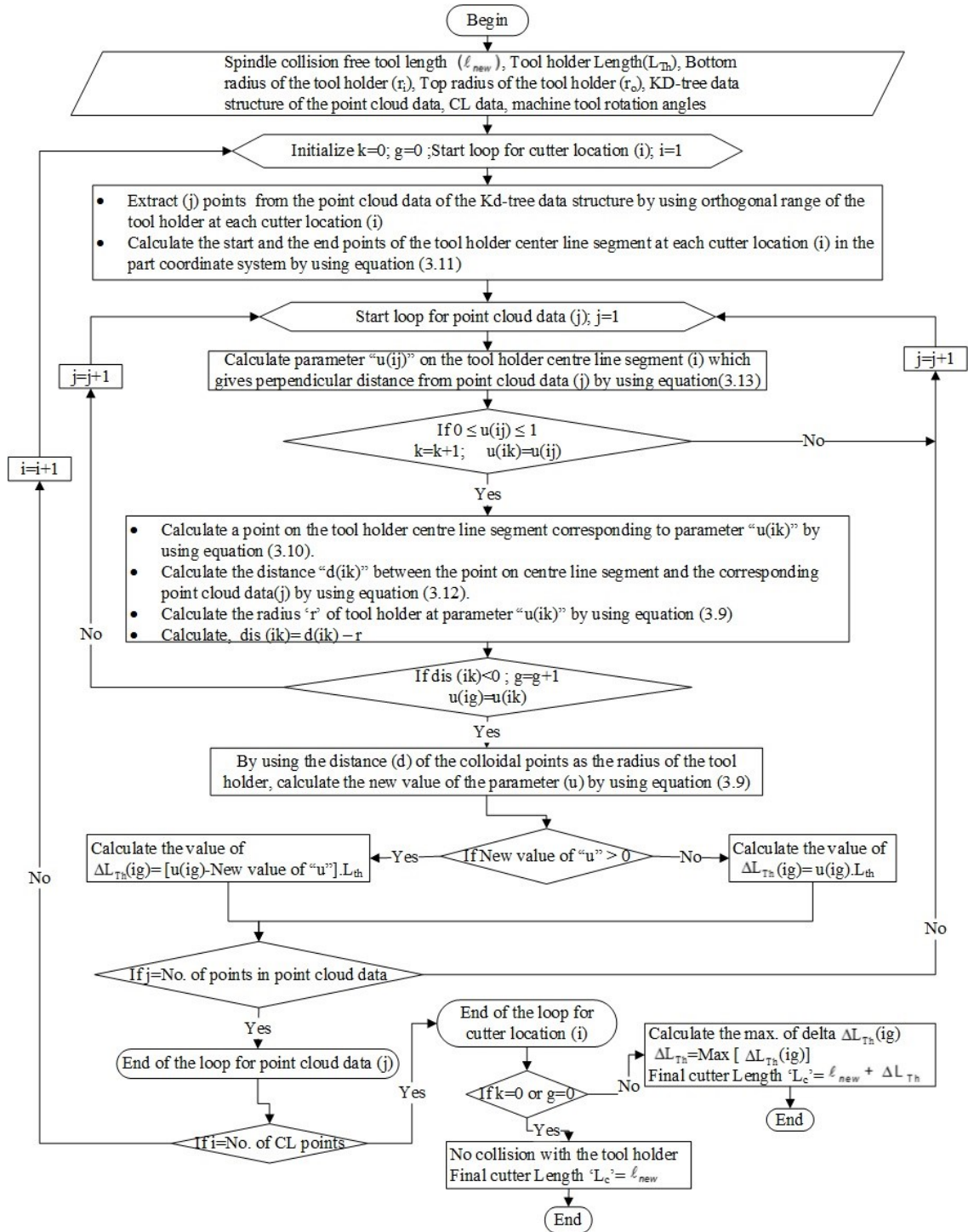


Figure 3.9- Flow chart of the algorithm for the tool holder collision detection and removal by the optimum cutter length

### 3.5 Applications

There are two main industrial applications of the proposed algorithm

1. For the given design of the tool holder, determination of the minimum overhang tool length for the complete machining of the design part on the five axis machine tools.
2. Determination of the overall cutting system length for the minimum overhang tool length and then on the basis of the overall cutting system length 5-axis machine tool working envelope can be evaluated.

Example of the collision detection and removal by the optimum length of the cutter at each cutter location during the machining of the work in process model along with the fixture is given below. Representation of the work in process model along with the fixture as a point cloud data with the density of 0.1 No. of points/mm<sup>2</sup> is shown in figure 3.10 (c).

**Table 3.1: Cutting system parameters**

$\ell$	Length of the tool at initial mounting position	40mm
$r_c$	Radius of the cutter	5mm
$L_{Th}$	Tool holder length	50mm
$r_{Th}^i$	Bottom radius of the tool holder or truncated cone	30mm
$r_{Th}^o$	Top radius of the tool holder or truncated cone	50mm
$L_s$	Spindle length	200mm
$r_s$	Spindle radius	120mm

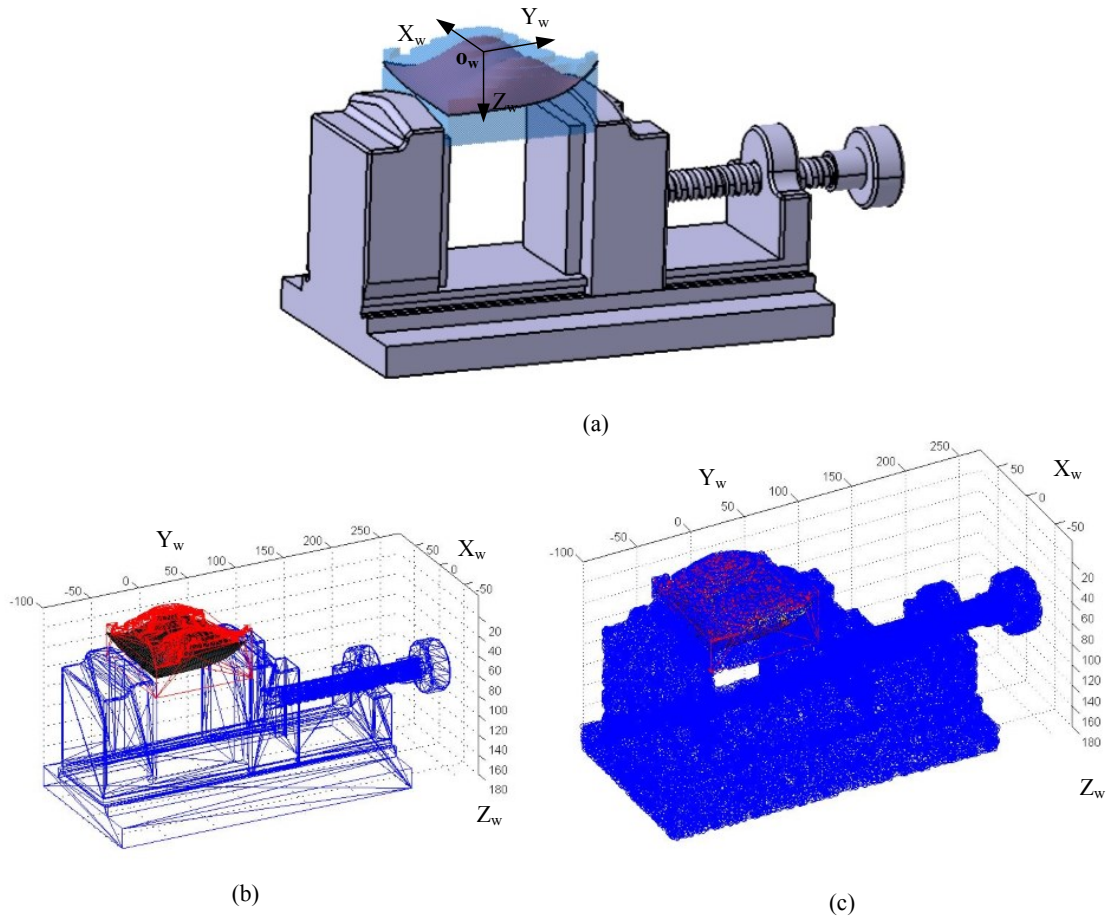


Figure 3.10-(a) Solid model (b) Triangular tessellation representation. (c) Point cloud data representation of the work in process model along with the fixture in part coordinate system.

### 3.5.1 Determination of the possible candidate points for the collision detection by the KD tree approach

Five axis tool paths are generated for the machining of the work in process model with 677 CL points and 32 tool passes. For the point cloud density of 0.1 points /mm<sup>2</sup>, 26393 and 4279 numbers of points are generated for the fixture and the work in process model respectively. Figure 3.11 and 3.12 shows the no. of possible candidate points at each cutter location out of 30672 points for the collision detection determined by the KD-tree

approach for the third tool path. First, at the initial tool length of  $l = 40\text{mm}$  orthogonal range of the spindle is determined at each cutter location of the third tool path and possible candidate points are found by Kd-tree approach. At the third tool path collision is detected with the spindle and it can be removed by the  $l_{new} = 56.4476\text{mm}$ . On the basis of the new tool length orthogonal range of the tool holder is determined at each cutter location and the possible candidate points are found by the Kd-tree approach.

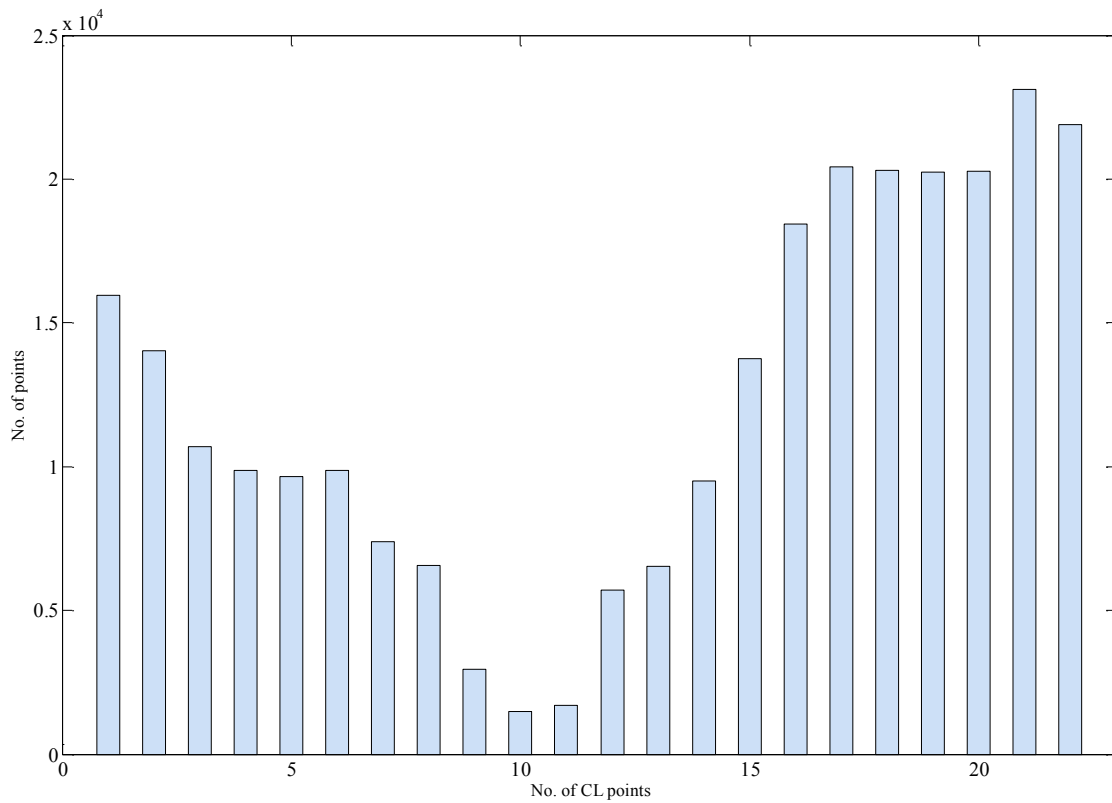


Figure 3.11-No. of points determined from the orthogonal range of spindle by Kd-tree structure of 30672 sample points, when tool length is 40mm.

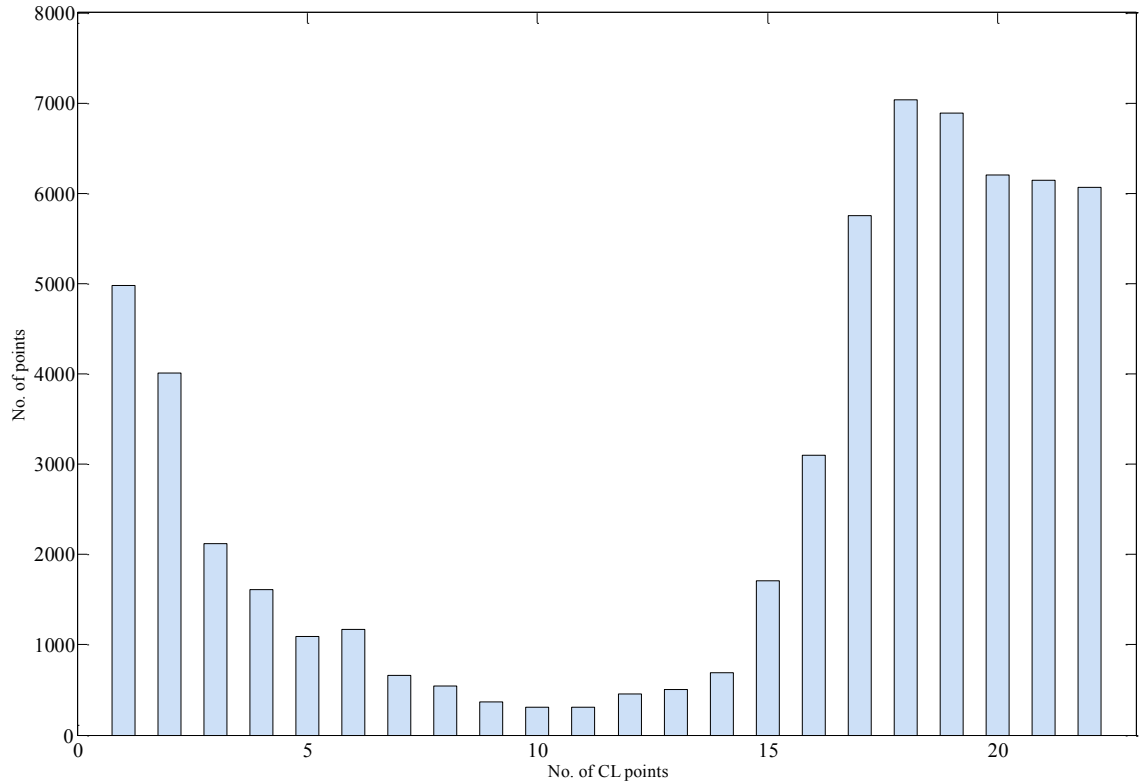


Figure 3.12- No. of points determined from the orthogonal range of the tool holder by Kd-tree structure of 30672 sample points, when tool length is 56.4476mm.

### 3.5.2 Results and simulation verification

For each tool path, the optimum length of the tool is calculated which can avoid the collision. At the second tool path, the optimum length is found 62.4611mm. This length is the largest length among the entire tool paths and could be used for the complete machining of the part. Following table shows the result at the 2<sup>nd</sup> tool path

**Table 3.2: Minimum cutter length needed at some colloidal cutter locations of 2<sup>nd</sup> tool path**

<i>Index no. of CL point</i>	16	17	18	20	Max.
For collision with spindle, change in length needed at each cutter location (mm)	1.4899	12.9065	22.4611	9.5921	22.4611
For collision with tool holder, change in length needed at each cutter location (mm)	0	0	0	0	0
Min. length needed to avoid collision at each CL point(mm)	40+1.4899 =41.4899	40+12.9065 =42.9065	40+22.4611 =62.4611	40+9.5921 =49.5921	62.4611

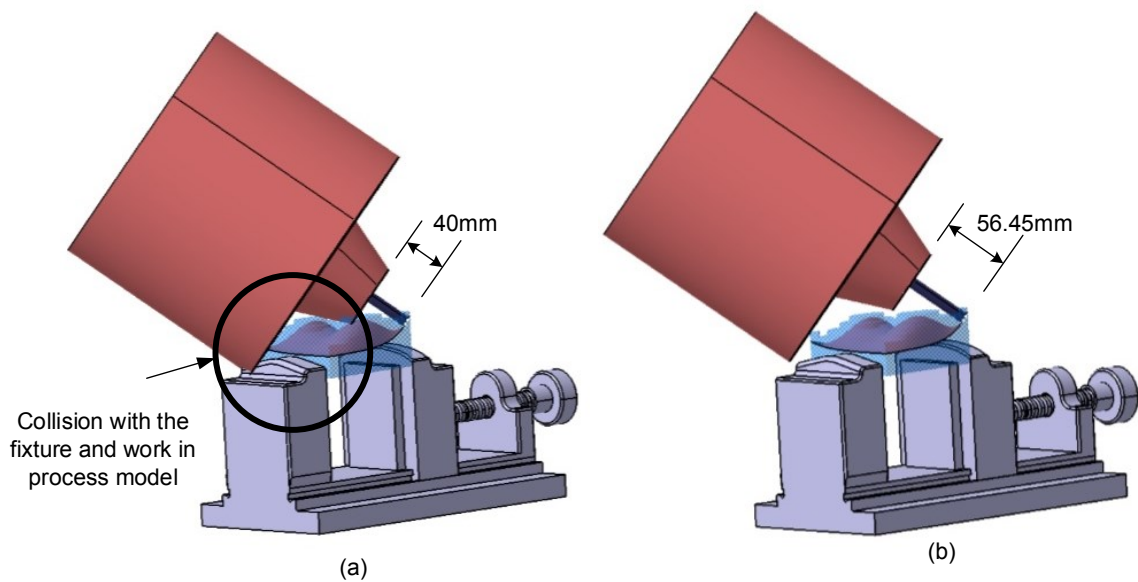


Figure 3.13- At 3<sup>rd</sup> tool path and 20<sup>th</sup> cutter location with machine rotations of C= -26.49° b=52.74°  
 (a) Collision of cutting system with the fixture and work in process model with tool length of 40mm. (b) No collision with the tool length of 56.45mm.

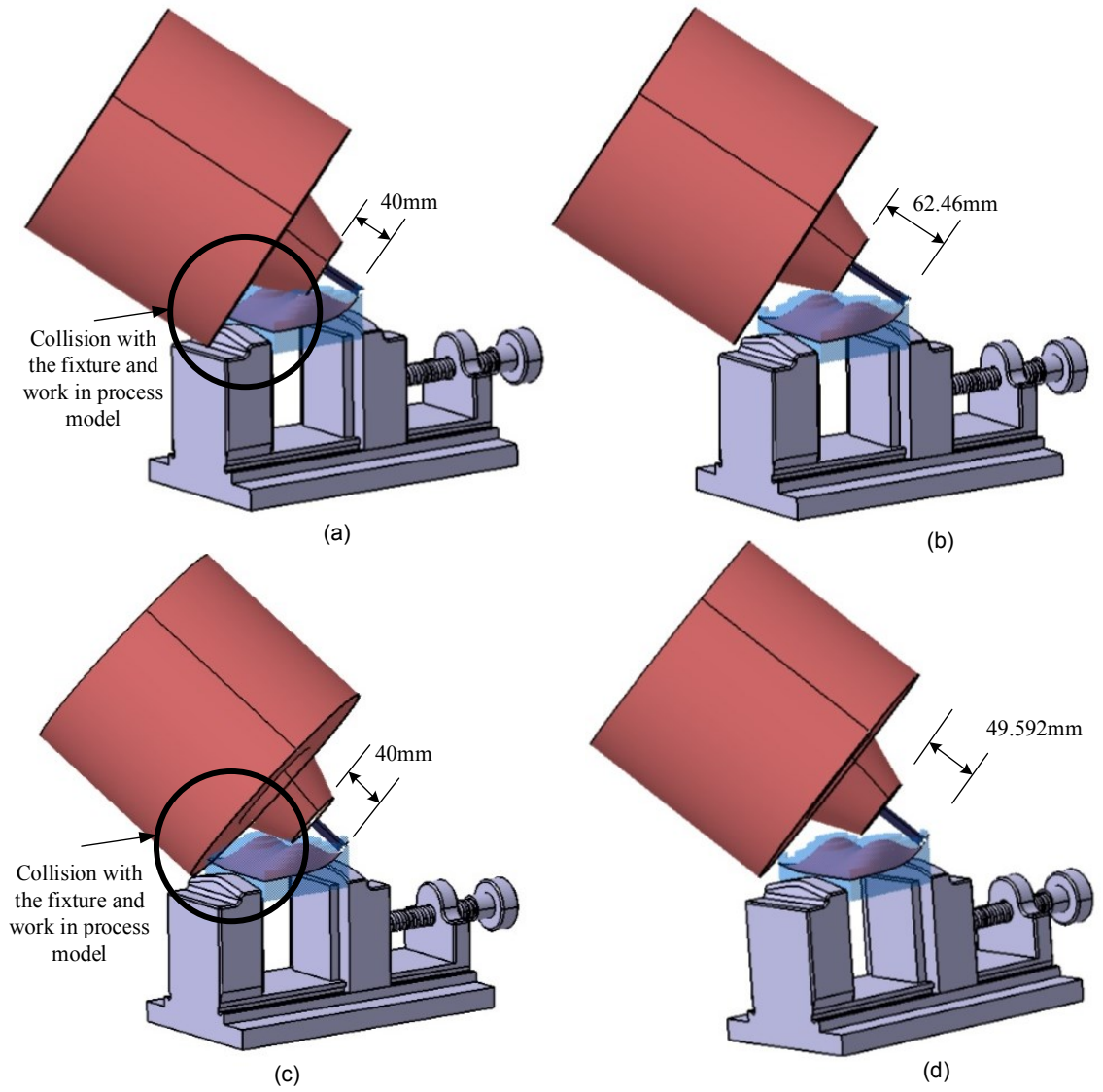


Figure 3. 14-(a) At 2<sup>nd</sup> tool path and 18<sup>th</sup> cutter location with machine rotations of  $C=-223.477^\circ$  and  $b=56.890^\circ$  collision of the cutting system with the tool length of 40mm. (b) No collision with the tool length of 62.46mm and (c) At 20<sup>th</sup> cutter location with machine rotations of  $C=-232.22^\circ$   $b=49.15^\circ$  collision of the cutting system with tool length of 40mm. (d) No collision with the tool length of 49.592mm.

Figure 3.13 and 3.14 shows the simulation verification at different cutter locations for 3<sup>rd</sup> and 2<sup>nd</sup> tool paths respectively. Collision due to the short tool length and collision avoidance with the optimum length can be seen clearly at different cutter locations.

### 3.6 Summary

A new and efficient algorithm for the avoidance of collision by the optimum cutter length has been proposed. Based on this algorithm, selection of the tool holder for the minimum overhang tool length among the different available tool holders is also possible. After getting the optimal cutter length, over all cutting system length can be determined and then working envelope of the 5-axis machine tool can be evaluated. The main features of this algorithm can be highlighted as under

- 1 Since the collision detection is based on the point cloud data of the fixture as well as the work in process model. Any design of the fixture can be used for the avoidance of the collision.
- 2 An efficient approach of Kd-tree data structure for searching possible candidates of the colloidal points of the fixture as well as work in process model with the cutting system is developed.
- 3 The method developed in this research is implemented on type 'C' 5-axis machine tools whose one rotary axis belongs to the table and the other one is attached with the spindle. For the other types of the configuration of the machine possible candidates for the collision may vary.
- 4 This method also provides the opportunity of selection the tool holder, which gives the shorter overhang length of the cutter or shorter overall cutting system length.

## Chapter 4

# **A Precise Approach for the Determination of the Setup Parameters to Utilize the Maximum Work Space of 5-Axis Machine Tools**

The maximum workspace utilization of the five axis machine tools is a critical task. Cutting system length determines the tool tip reachable workspace for the five axis machine tools. Setup parameters for the work piece mounting on the table can be chosen randomly for the post processing which do not give the guarantee for machining the part without over travel limits of the machine tools. In this research, a precise method is developed for the determination of the setup parameters for the work piece mounting on the table which guarantee the machining of the part without over travel limits. The proposed algorithm has the capability of doing the machining of the big parts in the minimum number of the setups.

The setup parameters for mounting the work piece on the table can be defined as the location of the origin of the part coordinate system in the table coordinate system and they are shown in figure 4.1. Besides the overall cutting system length, these setup parameters are also responsible of the machine tool translational over travel limits. These setup parameters should be selected prior to the machining in such a way that there is no machine tool translational over travel limits occurs.

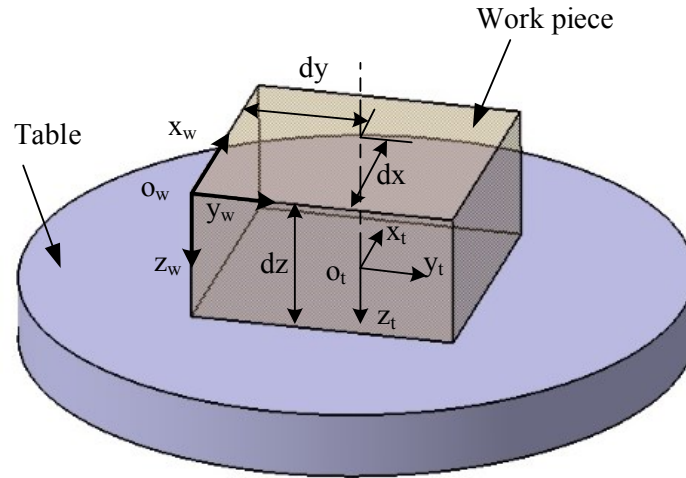


Figure 4.1- Standard setup parameters of a part on the machine table

In order to find the feasible set up parameters for mounting the work piece on the table, a generalized method is developed which can be applicable to any type of the five axis machine tool configuration. The table coordinate system in the kinematic chain can be selected as the reference coordinate system and the tool tip and the table accessible work space can be calculated in the table coordinate system. Once the tool tip and the table accessible work space is calculated in the table coordinate system, it is necessary for the cutter work piece engagement to calculate the location of the CL points in the table coordinate system and bound these cutter locations within the tool tip and the table accessible work space. The calculation of the tool tip and the table accessible work space may depend on the location of the translational axes. For example, if all the translational axes belong to the spindle then only tool tip accessible work space is needed in the table coordinate system. Overview of the method for finding the feasible setup parameters is presented with the help of the flow chart as shown in figure 4.2. The functions established

in this flow chart is for the DMU60-T machine tools but other functions can be developed for any other type of the configuration of the five-axis machine tools with the different independent variables.

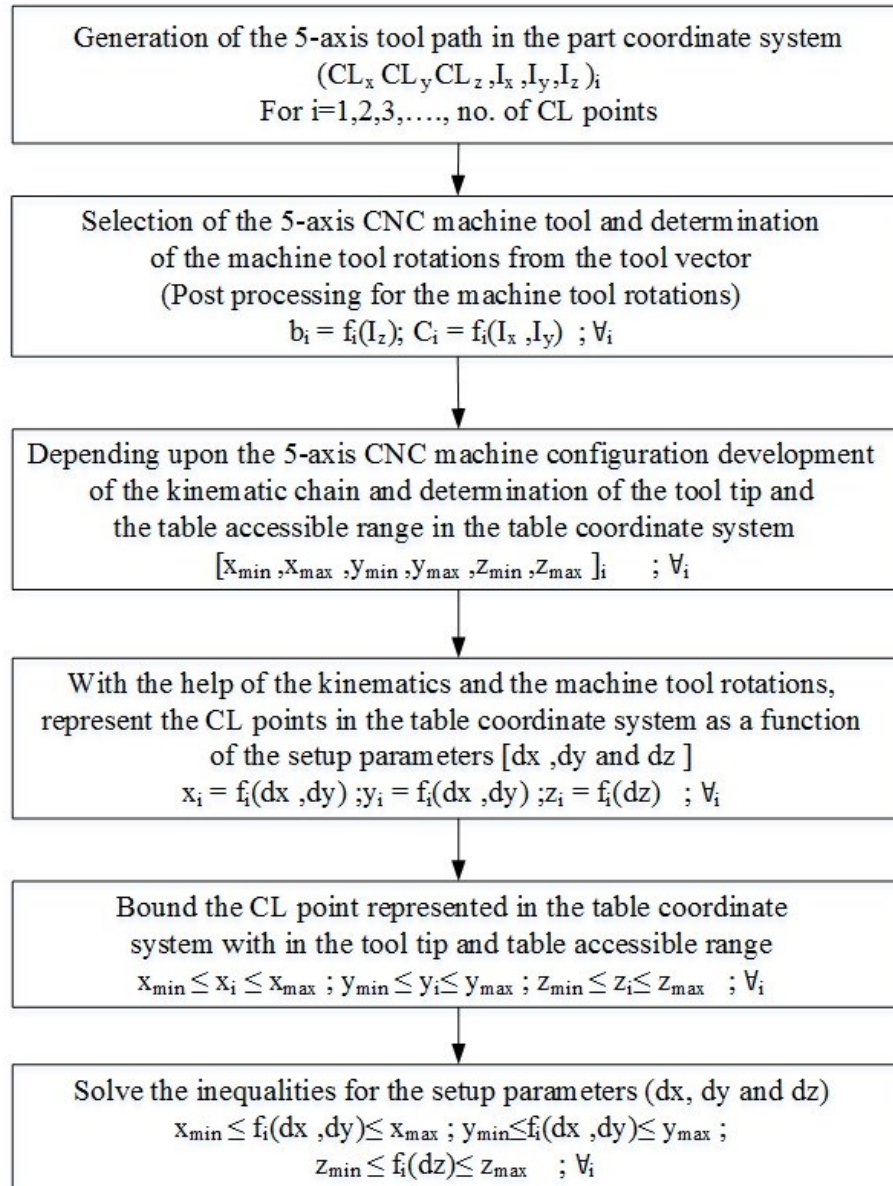


Figure 4.2- Basic methodology for finding the feasible setup parameters.

In order to follow the methodology presented in figure 4.2, this chapter is divided into five sections. In the section 1, setup parameters along with the kinematics of the 5-axis machine tools are discussed. In the section 2, the tool tip reachable work space is presented. A new mathematical model for the determination of the feasible region on the table for mounting the work piece is presented in section 3. In the fourth section table accessible work space is presented along with the determination of the setup height of the part ' $dz$ '. The last section concludes the research with the practical machining examples.

#### **4.1 Kinematics of the 5-axis machine tool**

A typical five axis machine has three translational axes and two rotary axes. Since the methodology developed in this chapter is implemented on the "C" type 5-axis machine tools, whose one rotary axis belongs to the table and the other is attached with spindle. The configuration of the machine along with the axes motion is already shown in figure 1.2.

Derivation of the machine coordinates can be accomplished by considering the three types of transformations.

1. Coordinate transformation to another reference system without motions.
2. Transformation corresponding to the actual machine rotations, and
3. Transformation corresponding to the actual machine translations.

The tool path (cutter locations and orientations) is generated in the part coordinate system ( $O_w$ ). Initially, origin of the cutter coordinate system coincides with the origin of



### 4.1.1 Derivation of the machine translational coordinates

Let “P<sub>w</sub>”  $\begin{bmatrix} CL_x & CL_y & CL_z & 1 \end{bmatrix}^T$  be a point in the part coordinate system.

Following steps are needed to transform “P<sub>w</sub>” from the part coordinate system (o<sub>w</sub>) to the cutter coordinate system (o<sub>c</sub>).

#### Step 1:

Map the point ‘P<sub>w</sub>’ in the o<sub>t</sub>-coordinate system.

$$P_t = T_1 \cdot P_w = \begin{bmatrix} 1 & 0 & 0 & dx \\ 0 & 1 & 0 & dy \\ 0 & 0 & 1 & dz \\ 0 & 0 & 0 & 1 \end{bmatrix} \cdot P_w$$

Where (dx dy dz) are the coordinates of the ‘o<sub>w</sub>’ in the o<sub>t</sub>-coordinate system and are called the setup parameters for mounting the work piece on the table.

#### Step 2:

Rotation around the z<sub>t</sub>-axis in ‘o<sub>t</sub>’ by the angle ‘C’. The point ‘P<sub>t</sub>’ is rotated around the z<sub>t</sub>-axis in the o<sub>t</sub>-coordinate system to a new location ‘P<sub>t</sub>’.

$$P'_t = T_2 \cdot P_t = \begin{bmatrix} \cos C & -\sin C & 0 & 0 \\ \sin C & \cos C & 0 & 0 \\ 0 & 0 & 1 & 0 \\ 0 & 0 & 0 & 1 \end{bmatrix} \cdot P_t$$

#### Step 3:

Before translating the point P<sub>t</sub> in the o<sub>p</sub>-coordinate system, it is necessary to transform the point P<sub>t</sub> in the other coordinate system ‘o<sub>l</sub>’ which has the same origin as the o<sub>t</sub>- coordinate system and has an orientation of the o<sub>p</sub>-coordinate system.

$$P_t'' = T_3 \cdot P_t' = \begin{bmatrix} 0 & 1 & 0 & 0 \\ 1 & 0 & 0 & 0 \\ 0 & 0 & -1 & 0 \\ 0 & 0 & 0 & 1 \end{bmatrix} \cdot P_t'$$

**Step 4:**

Translate the point ‘ $P_t''$ ’ in the  $o_p$ -coordinate system with the machine slide translation ‘ $M$ ’.

The work piece attached to the table will appear to move away from the spindle in the negative directions of the  $o_p$ -coordinate system for the positive value of the machine slide translation ‘ $M$ ’. Thus for machines slide translation  $M(x \ y \ Z)$ , the center of the  $o_1$ -coordinate system will be at the location of  $(-dx - x \ -dy - y \ -L_o + dz - Z)$  in the  $o_p$ -coordinate system.

$$P_p = T_6 \cdot P_t'' = \begin{bmatrix} 1 & 0 & 0 & -dx - x \\ 0 & 1 & 0 & -dy - y \\ 0 & 0 & 1 & -L_o + dz - Z \\ 0 & 0 & 0 & 1 \end{bmatrix} \cdot P_t''$$

Where  $(-dx \ -dy \ -L_o + dz)$  is the coordinate of the origin ‘ $o_1$ ’ in the  $o_p$ -coordinate system with respect to the machining zero position.

**Step 5:**

Rotation around the  $y_p$ -axis in the  $o_p$ -coordinate system by the angle ‘ $b$ ’. The point ‘ $P_p$ ’ is represented in the rotated coordinate system as a point  $P_p'$ .

$$P'_p = T_5 \cdot P_p = \begin{bmatrix} \cos b & 0 & -\sin b & 0 \\ 0 & 1 & 0 & 0 \\ \sin b & 0 & \cos b & 0 \\ 0 & 0 & 0 & 1 \end{bmatrix} \cdot P_p$$

**Step 6:**

Map the point  $P'_p$  in the cutter coordinate system 'oc'.

$$P_c = T_6 \cdot P'_p = \begin{bmatrix} 1 & 0 & 0 & 0 \\ 0 & 1 & 0 & 0 \\ 0 & 0 & 1 & L_o \\ 0 & 0 & 0 & 1 \end{bmatrix} \cdot P'_p$$

It is clear from the above steps; any point in the part coordinate system can be transformed in the cutter coordinate system by the following series of the transformations.

$$P_c = T_6 \cdot T_5 \cdot T_4 \cdot T_3 \cdot T_2 \cdot T_1 \cdot P_w \quad (4.1)$$

Each CL point in the part coordinate will be the origin of the cutter coordinate system during the machining. By substituting the  $P_c = [0 \ 0 \ 0 \ 1]^T$  in equation (4.1) and after simplification, the machine coordinates can be given as

$$x = CL_x \cdot \sin(C) + dy \cdot \cos(C) + CL_y \cdot \cos(C) + dx \cdot \sin(C) - dy + L_o \cdot \sin(b) \quad (4.2)$$

$$y = CL_x \cdot \cos(C) - dy \cdot \sin(C) - CL_y \cdot \sin(C) + dx \cdot \cos(C) - dx \quad (4.3)$$

$$Z = -CL_z - L_o + L_o \cdot \cos(b) \quad (4.4)$$

**4.1.2 Machine tool rotations**

The four set of the machine tool rotations (b and C) are possible for the given tool vector in the part coordinate system. For the post processing, it is necessary to find the

rotation angles first, then it is possible to calculate the machine translation motion from the equations 4.2 to 4.4. The explanation of four possible machine tool rotation solutions is given in the appendix A.

## 4.2 Tool tip accessible work space model

The tool tip reachable work space can be represented in the table coordinate system 'o<sub>t</sub>'. During the machining, for the each CL point there is a spindle rotation angle 'b' which can define a rectangular range in the table coordinate system. The pivot point 'o<sub>p</sub>' moves on the rectangular plane defined by the maximum and the minimum limits of x and y travel of the machine tool. The figure 4.4 shows the vertices (ABCD) of the rectangular plane which defines the x and y travel limits in the o<sub>t</sub>-coordinate system.

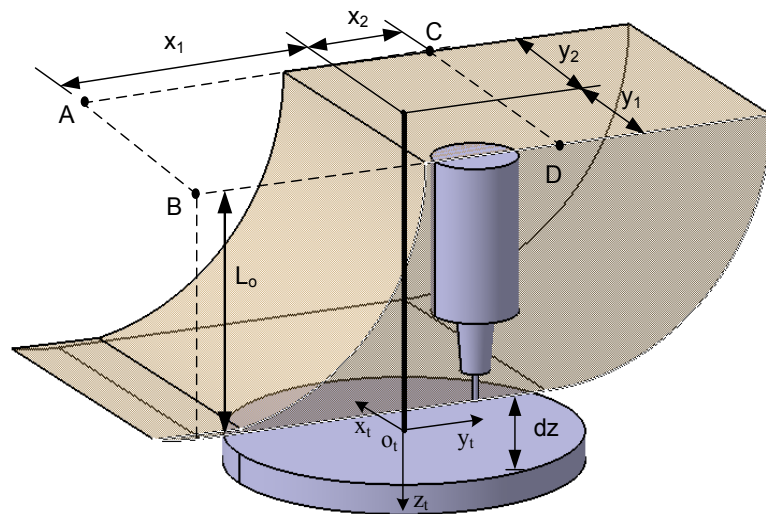


Figure 4.4- x and y travel limits in the table coordinate system 'o<sub>t</sub>'

For the DMU 60T 5-axis machine, table (4.1) shows the machine constant parameters. It depends on the machine tool structure and the similar machine constant parameters can be found for the other same configuration type DMU series such as the DMU 80T and the DMU 100T.

**Table 4. 1: Machine constant parameters for DMU 60 T**

S.NO	Machine constants	Description	Value (mm)
1	$x_1$	Min. x-travel limit from the origin of the table coordinate system ' $o_t$ '	500
2	$x_2$	Max. x-travel limit from the origin of the table coordinate system ' $o_t$ '	130
3	$y_1$	Min. y-travel limit from the origin of the table coordinate system ' $o_t$ '	280
4	$y_2$	Max. y-travel limit from the origin of the table coordinate system ' $o_t$ '	280

The overall cutting system length ' $L_o$ ' is also an important parameter for the tool tip rectangular range determination. For the given cutting system length and the tool rotation angle ( $\beta$ ), the tool tip rectangular range in the table coordinate system is constant.

#### 4.2.1 Unsymmetrical spindle rotation limits

The unsymmetrical spindle rotation limit also changes the rectangular range in the x-travel direction. The figures 4.5(a) and 4.5(b) shows the unsymmetrical spindle rotation limit along with the effect of the rectangular range in the x-travel direction.

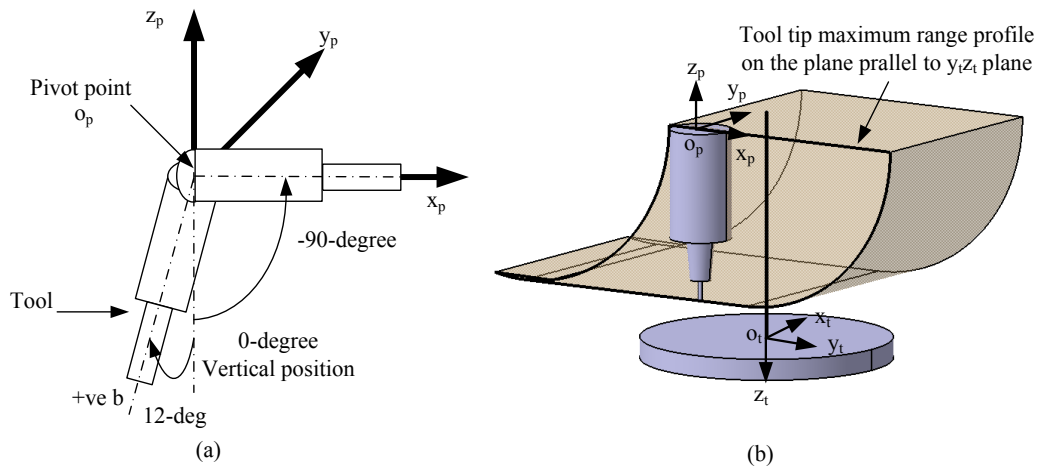


Figure 4. 5- (a) Unsymmetrical limits of spindle rotation & (b) Tool tip maximum range profile on the plane parallel to  $y_t z_t$ -plane.

It can be seen from the profile, minimum value of the ' $y_t$ ' coordinate of the tool tip limit in the table coordinate system ' $O_t$ ' initially decreases up to the  $12^\circ$  of the spindle rotation and then increases from  $-12^\circ$  to  $-90^\circ$ .

#### 4.2.2 Rectangular tool tip range in the table coordinate system

By using the machine constant parameters described in table 4.1, it is easy to define the rectangular range of the tool tip in the table coordinate system. Figure 4.6 shows the rectangular range for the constant overall cutting system length ' $L_o$ ' and the different values of the spindle rotation angle (b).

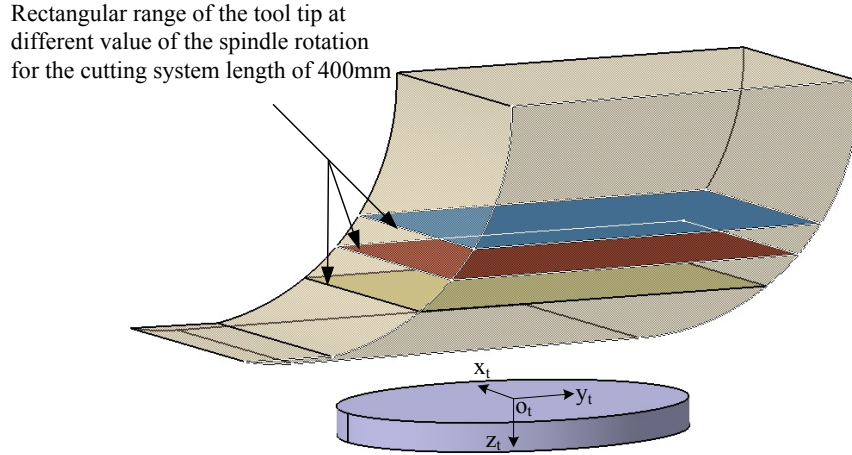


Figure 4. 6- Rectangular range for the different values of the spindle rotation

The equation of the quarter arc on the  $y_t z_t$ -plane of the table coordinate system with the radius of the overall cutting system length ( $L_o$ ) is given by

$$\begin{bmatrix} z_t(b) \\ y_t(b) \end{bmatrix} = \begin{bmatrix} L_o \cos(b) \\ -L_o \sin(b) \end{bmatrix} \quad 0 \leq b \leq -90^\circ \quad (4.5)$$

The equation of the right side tool tip arc in the table coordinate system can be generated by translating the equation (4.5) in the y-direction by ' $x_2=130\text{mm}$ ' and in the z-direction by ' $-dz-L_o$ '.

$$\begin{bmatrix} z_t'(b) \\ y_t'(b) \end{bmatrix} = \begin{bmatrix} L_o \cos(b) - dz - L_o \\ -L_o \sin(b) + 130 \end{bmatrix} \quad 0^\circ \leq b \leq -90^\circ \quad (4.6)$$

The maximum tool tip range along the  $y_t$ -direction is given by

$$y_{t(\max)}(b) = -L_o \sin(b) + 130 \quad 0^\circ \leq b \leq -90^\circ \quad (4.7)$$

Similarly, the minimum tool tip range along the  $y_t$ -direction is given by

$$y_{t(\min)}(b) = -L_o \cdot \sin(b) - 500 \quad 12^\circ \geq b \geq -90^\circ \quad (4.8)$$

The maximum and the minimum tool tip range along the  $x_t$ -direction are constant and are given by

$$x_{t(\min)} = -y_1 = -280 \quad (4.9)$$

$$x_{t(\max)} = y_2 = 280 \quad (4.10)$$

### **4.3 Mathematical model for the determination of the feasible region on the table for mounting the work piece based on the tool tip accessible work space**

The cutter work piece engagement at the certain CL point without  $x$  and  $y$  over travel limits of the machine tools depends on the setup parameters ‘ $dx$ ’ and ‘ $dy$ ’ as shown in figure 4.7. The rectangular range of the tool tip at some value of the spindle rotation angle ( $b$ ) is also shown in figure 4.7.

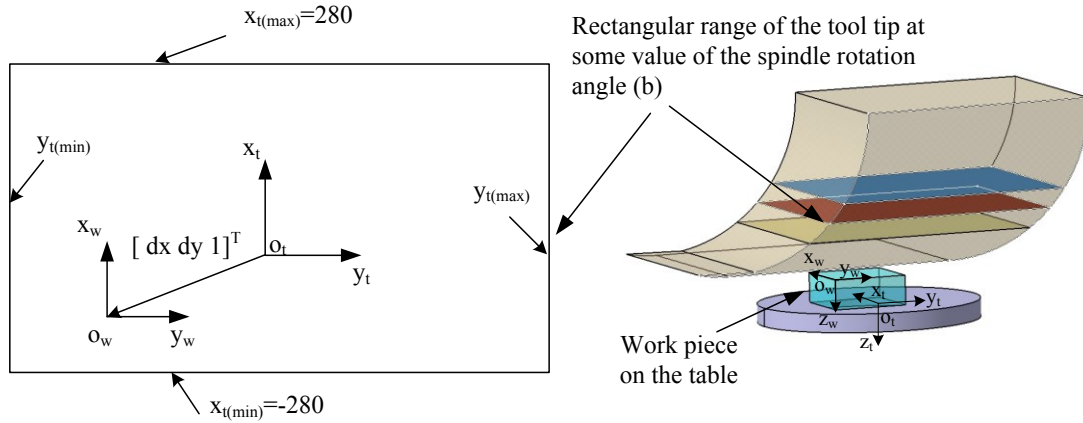


Figure 4.7- Rectangular range at some value of the spindle rotation along with the setup parameters.

Let  $[dx \ dy \ 1]^T$  be the coordinates describing the position of the work piece coordinate system in the table coordinate system. Any “CL” point in the work piece coordinate system can be mapped in the table coordinate system by the following translation matrix.

$$P_t = \begin{bmatrix} 1 & 0 & dx \\ 0 & 1 & dy \\ 0 & 0 & 1 \end{bmatrix} \cdot \begin{bmatrix} CL_x \\ CL_y \\ 1 \end{bmatrix}$$

After translation, the point ‘P<sub>t</sub>’ is rotated by the table rotation angle ‘C’ to the new location ‘P<sub>t</sub>’.

$$P'_t = \begin{bmatrix} \cos(C) & -\sin(C) & 0 \\ \sin(C) & \cos(C) & 0 \\ 0 & 0 & 1 \end{bmatrix} \begin{bmatrix} 1 & 0 & dx \\ 0 & 1 & dy \\ 0 & 0 & 1 \end{bmatrix} \cdot \begin{bmatrix} CL_x \\ CL_y \\ 1 \end{bmatrix}$$

After simplification, we get

$$\begin{bmatrix} x'_t \\ y'_t \end{bmatrix} = \begin{bmatrix} (CL_x + dx) \cdot \cos(C) - (CL_y + dy) \cdot \sin(C) \\ (CL_x + dx) \cdot \sin(C) + (CL_y + dy) \cdot \cos(C) \end{bmatrix} \quad (4.11)$$

The point  $P'_t = (x'_t \quad y'_t)$  is must be inside the rectangular range of the tool tip for the cutter work piece engagement or satisfying the following inequality

$$x_{t(\min)} \leq x'_t \leq x_{t(\max)}$$

$$y_{t(\min)} \leq y'_t \leq y_{t(\max)}$$

By substituting the values from the equations 4.7 to 4.11, we get

$$-280 \leq (CL_x + dx) \cdot \cos(C) - (CL_y + dy) \cdot \sin(C) \leq 280$$

$$-L_o \cdot \sin(b) - 500 \leq (CL_x + dx) \cdot \sin(C) + (CL_y + dy) \cdot \cos(C) \leq -L_o \cdot \sin(b) + 130$$

From the above two inequalities, we can derive the following four inequality functions

$$g_1(dx, dy) = (CL_x + dx) \cdot \cos(C) - (CL_y + dy) \cdot \sin(C) - 280 \leq 0$$

$$g_2(dx, dy) = (CL_x + dx) \cdot \cos(C) - (CL_y + dy) \cdot \sin(C) + 280 \geq 0$$

$$g_3(dx, dy) = (CL_x + dx) \cdot \sin(C) + (CL_y + dy) \cdot \cos(C) + L_o \cdot \sin(b) - 130 \leq 0$$

$$g_4(dx, dy) = (CL_x + dx) \cdot \sin(C) + (CL_y + dy) \cdot \cos(C) + L_o \cdot \sin(b) + 500 \geq 0$$

In order to find the feasible region for mounting the work piece on the table for each CL point, graphical approach [35] is applied. The common region for all the CL points

could be the final feasible region for selecting the setup parameters ‘ $dx$ ’ and ‘ $dy$ ’ of the work piece with respect to the table coordinate system.

#### 4.3.1 Model for generating the polygon of the feasible region

Consider the following inequality functions for each CL point

$$g_{1,k}(dx, dy) = (CL_{x,k} + dx) \cdot \cos(C_k) - (CL_{y,k} + dy) \cdot \sin(C_k) - 280 \leq 0$$

$$g_{2,k}(dx, dy) = (CL_{x,k} + dx) \cdot \cos(C_k) - (CL_{y,k} + dy) \cdot \sin(C_k) + 280 \geq 0$$

$$g_{3,k}(dx, dy) = (CL_{x,k} + dx) \cdot \sin(C_k) + (CL_{y,k} + dy) \cdot \cos(C_k) + L_o \cdot \sin(b_k) - 130 \leq 0$$

$$g_{4,k}(dx, dy) = (CL_{x,k} + dx) \cdot \sin(C_k) + (CL_{y,k} + dy) \cdot \cos(C_k) + L_o \cdot \sin(b_k) + 500 \geq 0$$

Where  $k=1, 2, 3, 4 \dots\dots\dots$ , No of CL points

$$\text{and } g_t(dx, dy) \in \{g_{1,k}(dx, dy), g_{2,k}(dx, dy), g_{3,k}(dx, dy), g_{4,k}(dx, dy)\}$$

Where  $t=1, 2, 3, 4 \dots\dots\dots$ , total no. of inequality functions (4x No. of CL points)

The following function lines are always parallel to each other for the each CL point because they have the equal coefficients of ‘ $dx$ ’ and ‘ $dy$ ’. Therefore,

$$g_{1,k}(dx, dy) = 0 \text{ is parallel to } g_{2,k}(dx, dy) = 0, \text{ and}$$

$$g_{3,k}(dx, dy) = 0 \text{ is parallel to } g_{4,k}(dx, dy) = 0$$

Initially, four intersection points are calculated from intersecting lines of the first CL point. These four points formed the edges of the rhombus. In order to get the parametric

equations of the edges of the rhombus, it is necessary to arrange the points in the clockwise or in the anticlockwise manner.

**(a) Mathematical model for the arrangement of the points describing the edges of the polygon:**

Let 'S' be the set of 2D points describing the vertices of the polygon

$$S = \{P(dx_n \quad dy_n)\}$$

Where  $n = 1, 2, 3 \dots$  No. of vertices of the polygon

The vertices can be arranged in the anticlockwise manner by arranging the ' $\theta_i$ ' in the ascending order as shown in figure 4.8 (c) and ' $\theta_i$ ' can be calculated as follows

$$\theta_i = \cos^{-1} \frac{(\hat{a} \cdot \vec{v}_i)}{|\vec{v}_i|}$$

for  $i = 1, 2, 3 \dots n - 1$

Where  $\vec{v}_i = \overline{P_0 P_i}$  is the vector from the lower left point 'P<sub>0</sub>' to the remaining points of the

set 'S' and  $\hat{a} = [1 \quad 0]^T$  is the unit vector along the positive x-axis direction

For the vertices  $P_1, P_2, P_3 \dots P_n$  arranged in the anticlockwise manner, the parametric equations of the edges of the polygon can be given as

$$l_i = P_i + v \cdot (P_{i+1} - P_i)$$

.....

.....

$$l_n = P_n + v \cdot (P_1 - P_n)$$

for  $i = 1, 2, 3, \dots, n$  and  $0 \leq v \leq 1$

The figure 4.8 shows the formation of polygon edges for  $n=5$  (No. of vertices)

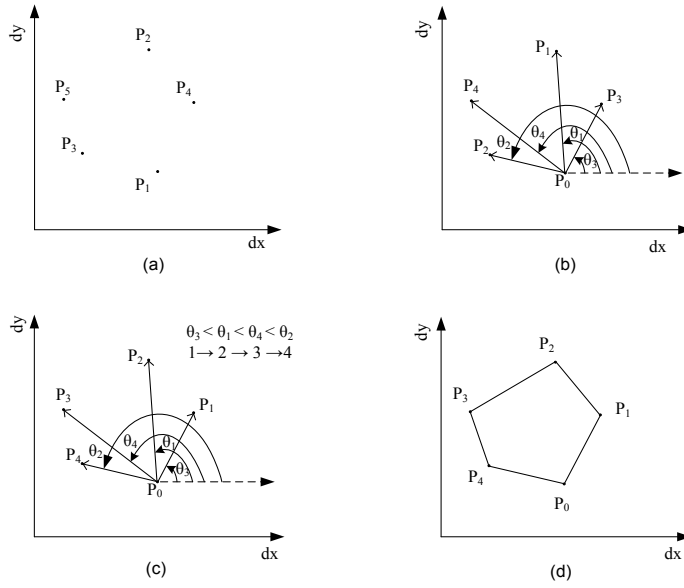


Figure 4.8- (a) Randomly named five vertices of the polygon. (b) Angles measured between the x-axis and the different vectors from the lower left point to the other vertices of the polygon (c) Points arrangement according the ascending order of the 'θ' (d) Final polygon.

After getting the four vertices and the parametric equations of the four edges for the first CL point, it is necessary to check polygon of the feasible region for the remaining inequalities functions.

**(b) Mathematical model for generating the final feasible polygon**

Any inequality function  $g_i(dx, dy)$  can have one of the three types of effect on the feasible polygon region.

$$FR_L \cap FR_p = \emptyset \tag{4.12}$$

$$FR_L \cap FR_p = FR_p \tag{4.13}$$

$$FR_L \cap FR_p = FR_p \quad (4.14)$$

Where  $FR_L$  = Feasible region specified by the inequality function  $g_i(dx, dy)$

$FR_p$  = Feasible region bounded by the polygon

$FR_{p'}$  = Feasible region bounded by the reduced size polygon

From the equation (4.12), it can be seen that there is no feasible region for finding the parameters 'dx' and 'dy' for mounting the work piece on the table. This case is shown in figure 4.9.

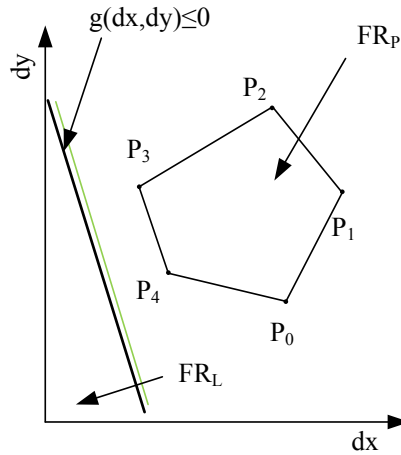


Figure 4.9- No feasible region case when  $FR_L \cap FR_p = \emptyset$

From equation (4.13), it can be seen that existing feasible region of the polygon will remain same after applying the inequality function. Figure 4.10 shows the three cases which satisfying equation (4.13)

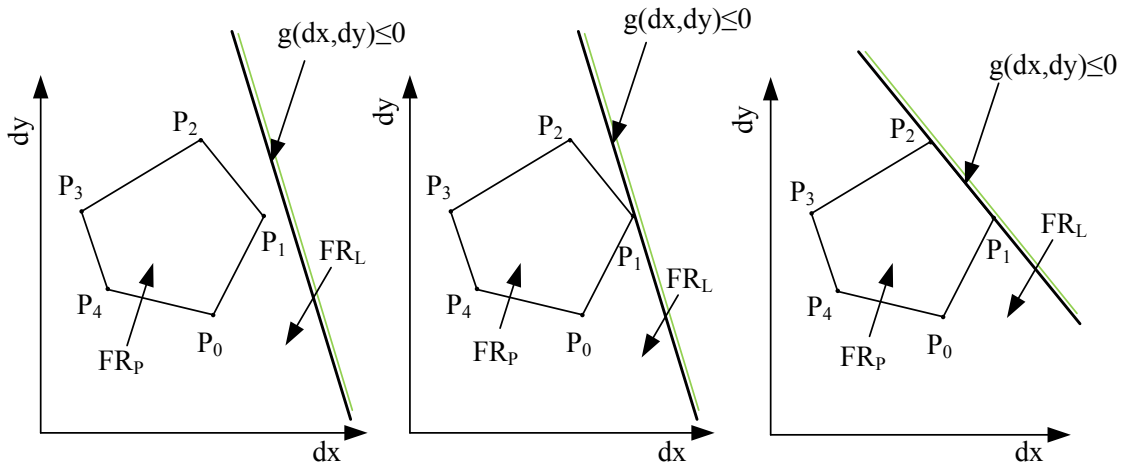


Figure 4.10- No change in the feasible region when inequality function is applied or when  $FR_L \cap FR_p = FR_p$

From equation (4.14), it can be seen that the inequality function reduces the area of the feasible polygon. Figure 4.11 shows the two cases which satisfying the equation (4.14)

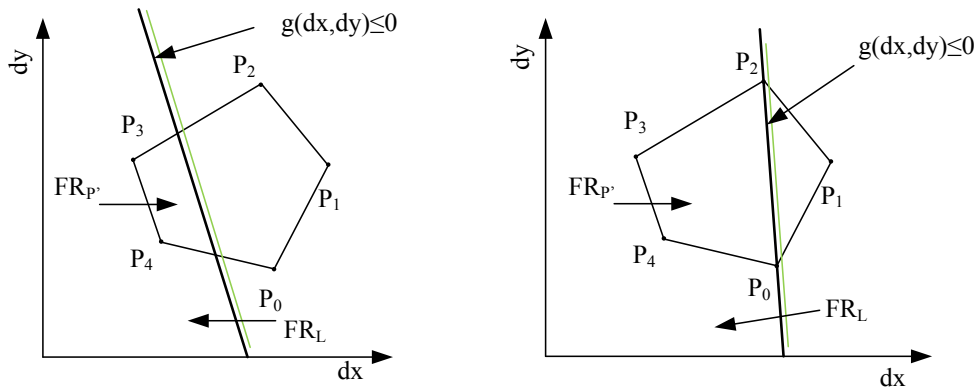


Figure 4.11- Reduction in the feasible region when inequality function is applied or when  $FR_L \cap FR_p = FR_p$ .

To get the final feasible polygon it is necessary to calculate the parametric value on the edges of the polygon for the intersection of the edges with the parametric line of the inequality function and it can be calculated as

$$v = \frac{(dx_2 - dx_1) \cdot (dy_1 - dy_i) + (dx_i - dx_1) \cdot (dy_2 - dy_1)}{(dx_2 - dx_1) \cdot (dy_{i+1} - dy_i) - (dx_{i+1} - dx_i) \cdot (dy_2 - dy_1)} \quad \text{for } 0 \leq v \leq 1$$

Where  $P_1 = (dx_1 \quad dy_1)$  and  $P_2 = (dx_2 \quad dy_2)$  are the end point of the inequality function and  $P_i = (dx_i \quad dy_i)$  &  $P_{i+1} = (dx_{i+1} \quad dy_{i+1})$  are the end points of the edge ' $l_i$ ' of the polygon

#### **4.4 Determination of the feasible 'dz' parameter of mounting the work piece on the table**

The two setup parameters ' $dx$ ' and ' $dy$ ' are defined the over travel limits of the spindle and can be determined by using the method described in section 4.3. The ' $dz$ ' parameter defines the over travel limit of the table. Figure 4.12 describes the table travel limits with respect to the  $x_p y_p$ -plane of the ' $o_p$ ' coordinate system at the machining zero position.

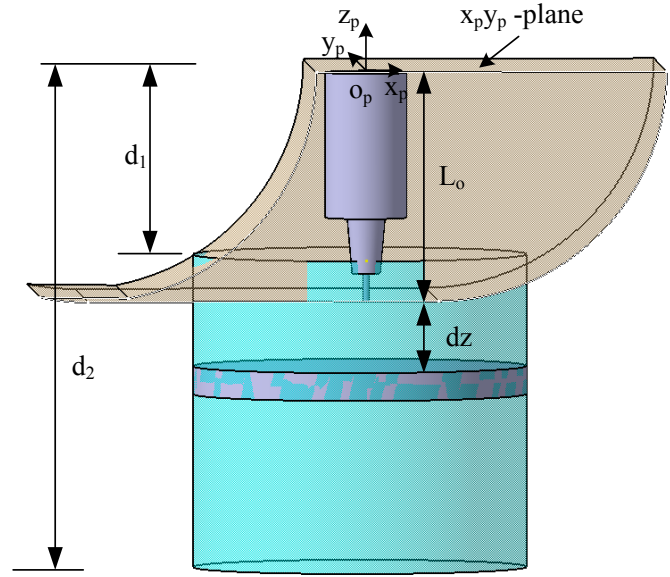


Figure 4.12- Table travel limit along with the machine constants  $d_1$  and  $d_2$

The machine constants  $d_1$  and  $d_2$  can be defined as follows along with their values for DMU 60T machine tools

$d_1$ = Distance between the  $x_p y_p$ -plane and the table maximum height position=338mm

$d_2$ = Distance between the  $x_p y_p$ -plane and the table minimum height position.

$d_2 = d_1 + \text{Overll z-travel limit} = 338+560 =898\text{mm}$

It is clear from figure (4.12) during the machining for each CL point; z-travel of the table should satisfy the following inequality

$$-(L_o + dz - d_1) \leq Z\text{-travel of the table} \leq (d_2 - dz - L_o)$$

By substituting the value of the Z-travel of the table from equation (4.4), we get

$$(d_1 - L_o - dz) \leq (L_o \cdot \cos(b) - CL_z - L_o) \leq (d_2 - dz - L_o)$$

$$\text{and, } \text{Max}(d_1 - L_o \cdot \cos(b_k) + CL_{z,k}) \leq dz \leq \text{Min}(d_2 - L_o \cdot \cos(b_k) + CL_{z,k}) \quad (4.15)$$

Where  $k=1, 2, 3, 4 \dots\dots\dots$  , No of CL points

The value of the 'dz' parameter must satisfy equation (4.15) to do the machining without over travel limit of the table.

#### **4.5 Machining examples along with the simulation verification**

For generating the tool path in the part coordinate system different machining strategies can be applied. The proposed method of determining the setup parameters for mounting the work piece on the table is based on the predetermined 5-axis machining tool path generated by the software such as CATIA. In the following section three machining examples are presented. First example is related with the machining of the simple prismatic part, the second example is also the prismatic part contain more features of the machining and third is the machining of the bracket for holding the pipe which includes some features of the continuous 5-axis machining. It can be seen clearly, for the bigger parts there is a small feasible polygon area for selecting the setup parameters. Furthermore, in the second example, there is also the possibility of obtaining two or more than two sets of the feasible regions for selecting the setup parameters.

##### **4.5.1 Prismatic part machining with two machining processes**

In this simple example, only two machining processes are required to complete the machining of the part. To show the effectiveness of the method bigger design part is selected. The size of the rough stock is  $(500 \times 450 \times 100) \text{ mm}^3$ . One side dimension (500mm) is close to the diameter (580mm) of the DMU 60T table.

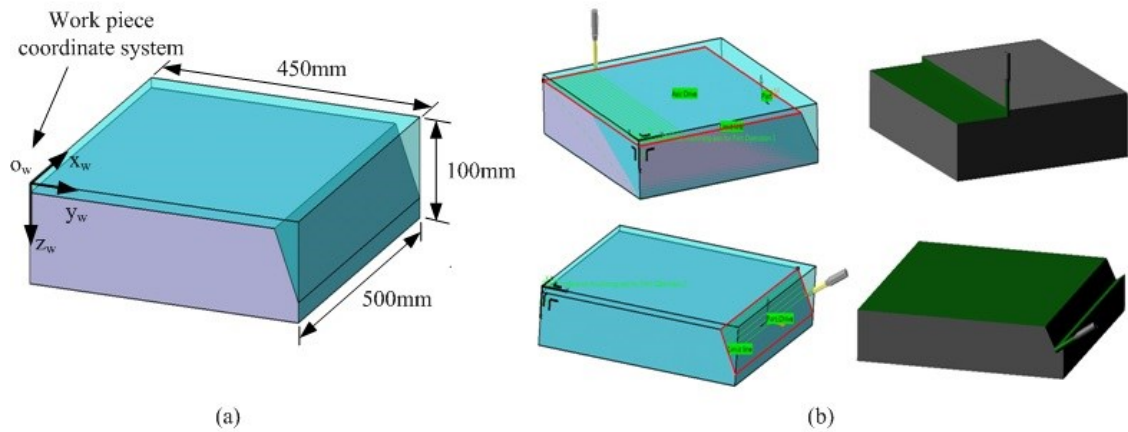


Figure 4.13- (a) Design part with the rough stock. (b) Tool path generation snap shots

Figure 4.13(a) shows the rough stock with the design part and the snap shot of two machining processes are shown in figure 4.13(b). The tool path is generated in such a way that tool axis is always normal to the design surface. After generating the tool path, CL points and tool vectors are generated in the work piece coordinate system. For the machine tool orientations (post processing), facing of the top surface can be done with  $b=0\text{deg}$  and  $C=0\text{deg}$  and inclined facing can be accomplished with  $b=-60\text{deg}$  and  $C=180\text{deg}$ . With the overall cutting system length ( $L_o=400\text{mm}$ ), feasible region for selecting  $dx$  and  $dy$  setup parameters for mounting the work piece on the table is shown in figure 4.14 (a). Setup of the stock on the table with the feasible setup parameters is shown in figure 4.14 (b) and it can also be seen that coordinates of the ' $o_w$ ' in the table coordinate system ' $o_t$ ' is  $(dx \quad dy \quad dz) = (-260 \quad -300 \quad -250)$ .

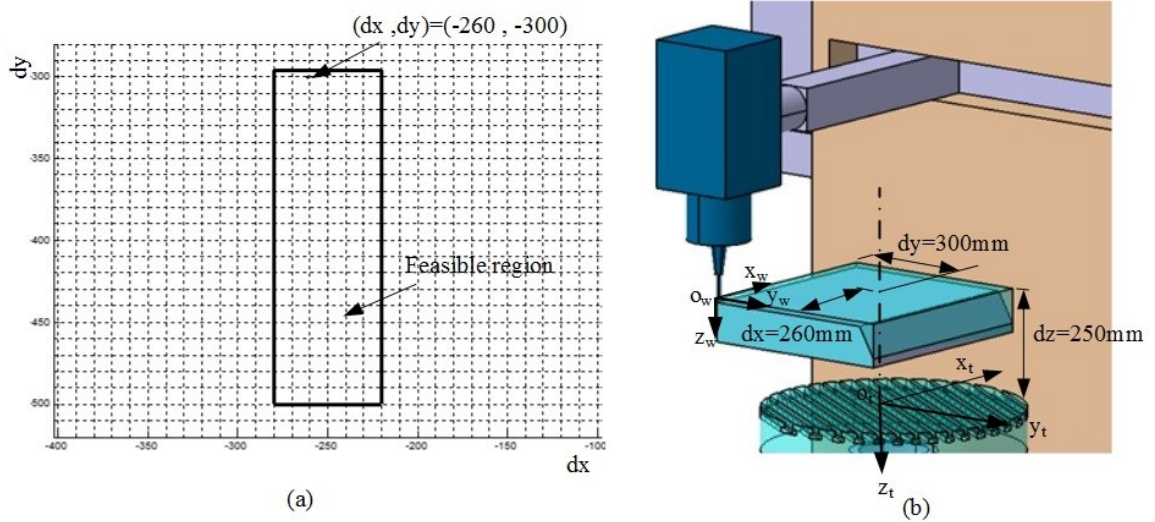


Figure 4.14- (a) Feasible region for selecting the setup parameters. (b) Example of setup the part when setup parameters are selected within the feasible region

To avoid the z-over travel limit of the table, it is necessary to setup the part at the certain height 'dz'. This height gives the room for placing the fixture on which part is mounted and should satisfy the inequality (4.15). For the above example inequality (4.15) gives the result as

$$217.82 \leq dz \leq 508.00$$

In the figure 4.14 (b), dz=250mm is the safe value for machining the part without over travel of the z-travel limit. After selecting the feasible setup parameters, post processing (G-codes) are developed with the help of the equations presented in section-2 and the simulation of the machining shows that the part can be machined without over travel limits of the machine tool axes. In figure 4.15 (a) setup parameters  $(dx \ dy \ dz) = (-260 \ -280 \ -250)$  is shown and from figure 4.14 (a) it can be seen that  $(dx \ dy) = (-260 \ -280)$  is at the outside of the feasible region. G-codes are

generated with the setup parameters as shown in figure 4.15 (a) and the snap shot of the simulation of the machining in figure 4.15 (b) shows that some area of the design part (inclined surface) cannot be machine due to the machine x-travel limitation.

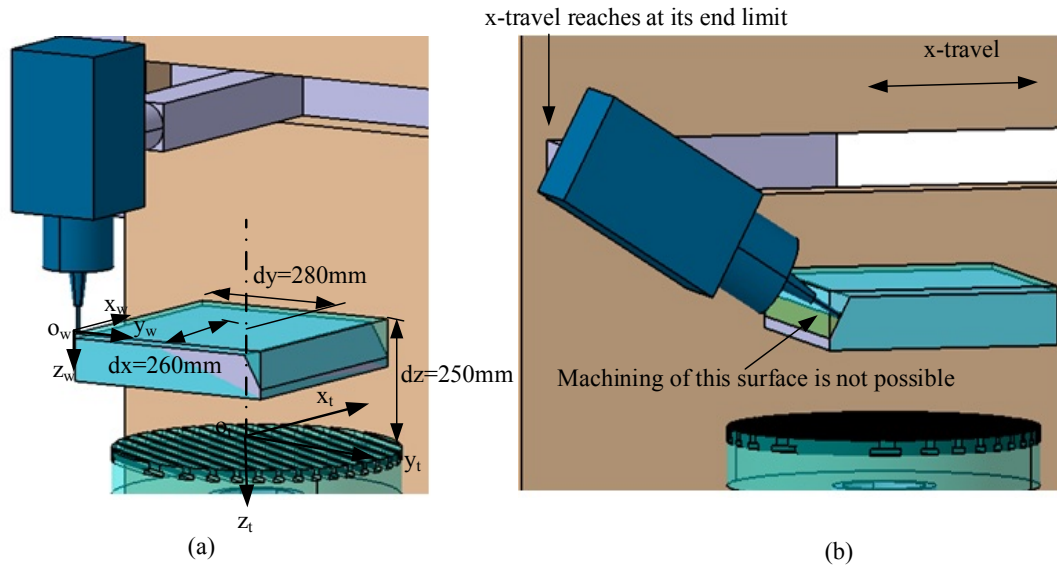


Figure 4.15- (a) Setup of the part when setup parameters are selected from outside the feasible region (b) Snap shot of the simulation showing that further machining is not possible due to the limitation of the x-travel

#### 4.5.2 Prismatic part machining with multiple machining processes

Another example of a prismatic part with multiple machining processes will be presented. The rough stock and the design part is shown in figure 4.16. The tool path is generated in such a way that the tool vector is always normal to the design surface. The snap shots of the top facing and four corners inclined facing are shown in figure 4.17 and 4.18 respectively.

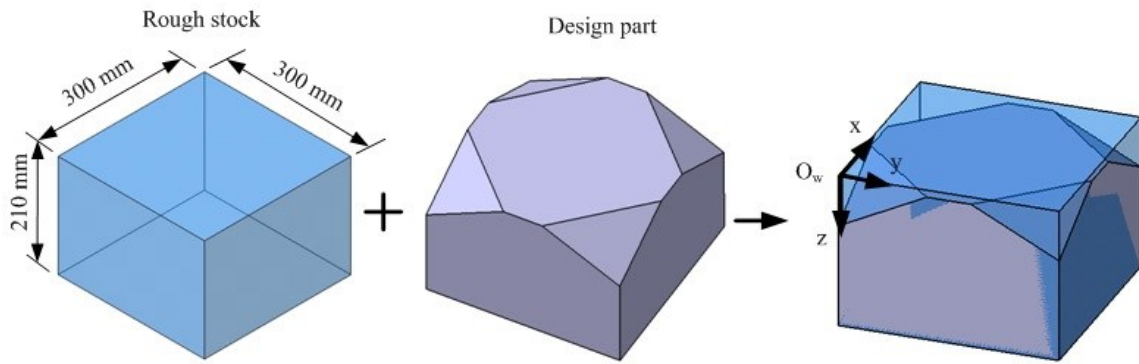


Figure 4.16-Design part and the rough stock

Five axis machining is an efficient way to remove the material from the inclined surface. If we use three axis machine instead of five axis, we need to design the fixture to hold the work piece for the four inclined faces. It also increases the setup time. For the post processing of the five axis machining, top facing is done with the rotations of  $C=0^\circ$  and  $b=0^\circ$  and the facing of the other four corners is conducted with  $b=-35.26^\circ$ . For the table rotation 'C', four times indexing is needed with the difference of  $90^\circ$ .

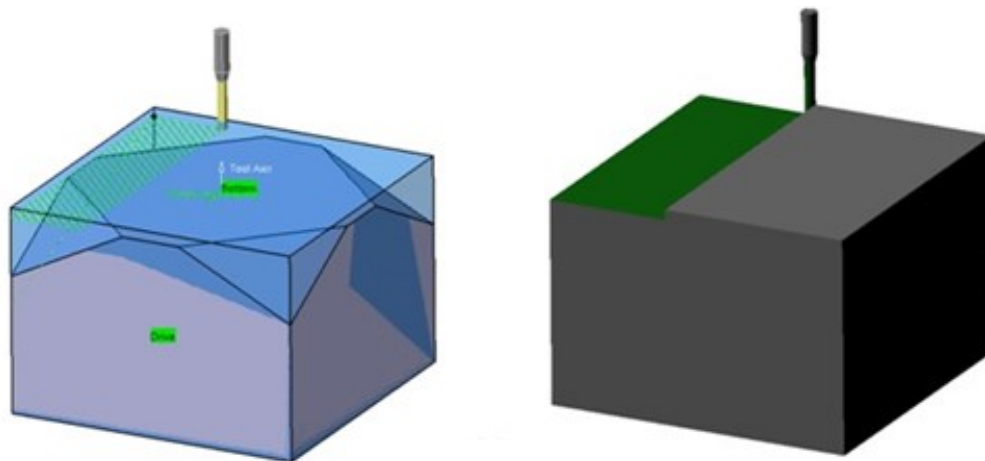


Figure 4.17-Snap shot of the top facing

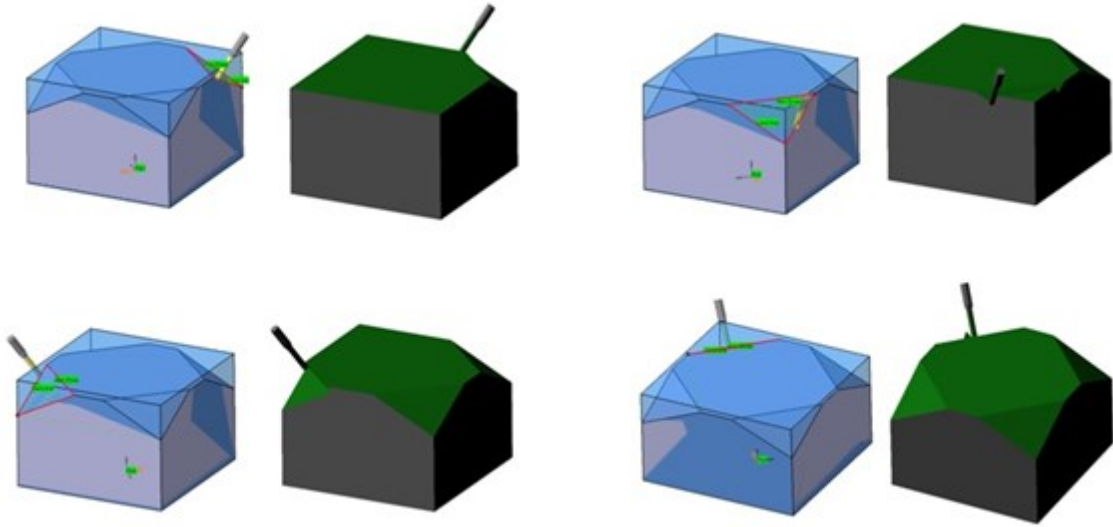


Figure 4.18-Snap shot of the four corners inclined facing

With the overall cutting system length of 400mm, five feasible regions for the determination of  $dx$  and  $dy$  setup parameters for the five different processing of the machining (one horizontal top facing and four corner inclined facing) are plotted and a common region among them as shown in figure 4.19 is the final feasible region for the determination of the setup parameters ( $dx$  and  $dy$ ). By choosing these parameters from the final feasible region, all five machining operations can be accomplished with a single setup and without over travel of the  $x$  and  $y$  axes of the machine tools. If the size of the part is bigger and the machining is not possible with the single setup then this method can also provide the choices of selecting the setup parameters ' $dx$ ' and ' $dy$ ' from the common region of two or more than two sets of the feasible regions. In other words, machining of the complete part can be possible with two or more than two setups.

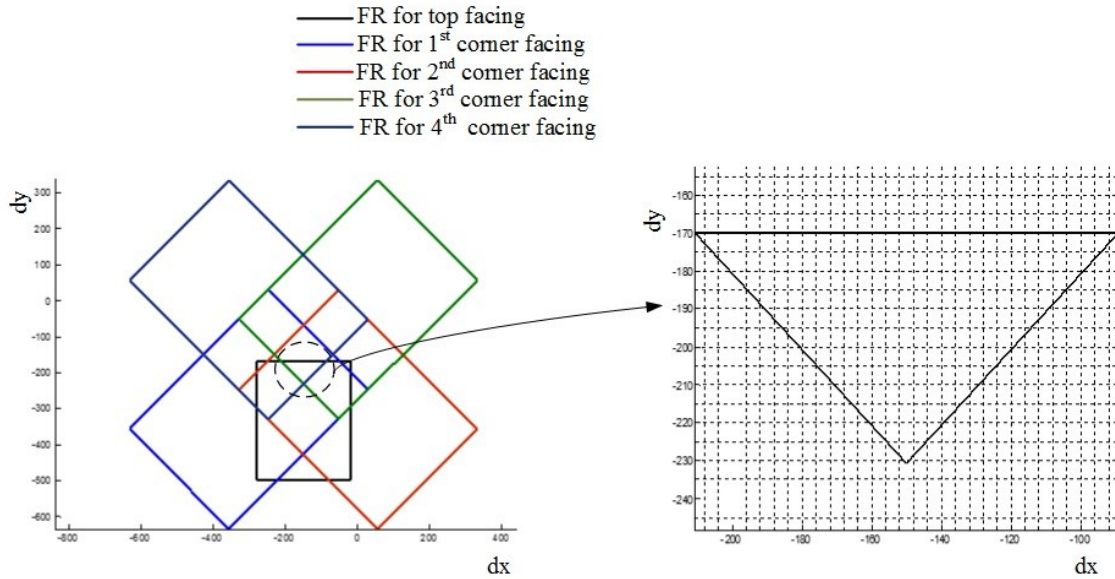


Figure 4.19-Five feasible regions for five machining processes along with the final common feasible region.

For the determination of the ‘dz’ setup parameter for this example, inequality 4.15 gives the following result.

$$81.33 \leq dz \leq 508.00 \quad (4.16)$$

Feasible setup parameters dx and dy can be selected from the final feasible region shown in figure 4.18 and the feasible ‘dz’ value can be selected from inequality 4.16. Two setups of the part on the table are shown in figure 4.20 and 4.21. One setup with  $(dx \ dy \ dz) = (-100 \ -175 \ -310)$  is shown in figure 4.19 along with the location of the  $(dx \ dy) = (-100 \ -175)$  in the final feasible region. With these parameters G-codes are generated and the simulation is conducted with the help of CATIA. In the simulation it can be seen that part can be machined completely without over travel limits of the machine translational axes.

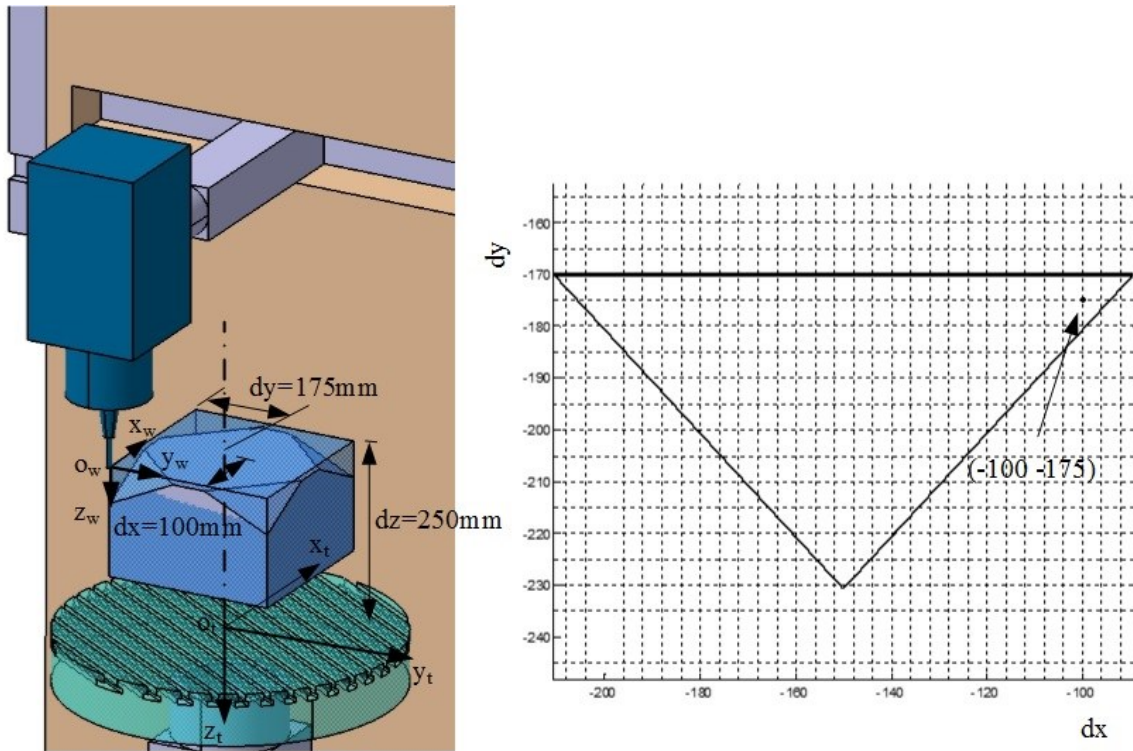


Figure 4.20- Feasible setup of the part on the machine table along with the location of the feasible point inside the final feasible region

Other setup with the setup parameters of  $(dx \ dy \ dz) = (-100 \ -190 \ -310)$  is shown in figure-4.20 along with the location of the  $(dx \ dy) = (-100 \ -190)$  in the graph of the final feasible region. In this figure it can be seen clearly that the selected parameters of  $dx$  and  $dy$  are located outside from the final feasible region. After generating the G-codes for the machine tool axes motion commands, simulation of the machining is done in CATIA. The simulation result shows that with these setup parameters all five machining processes cannot be completed and the some portion of the forth corner facing cannot be machined due to the travel limitation of the  $x$ -axis of the machine tools.

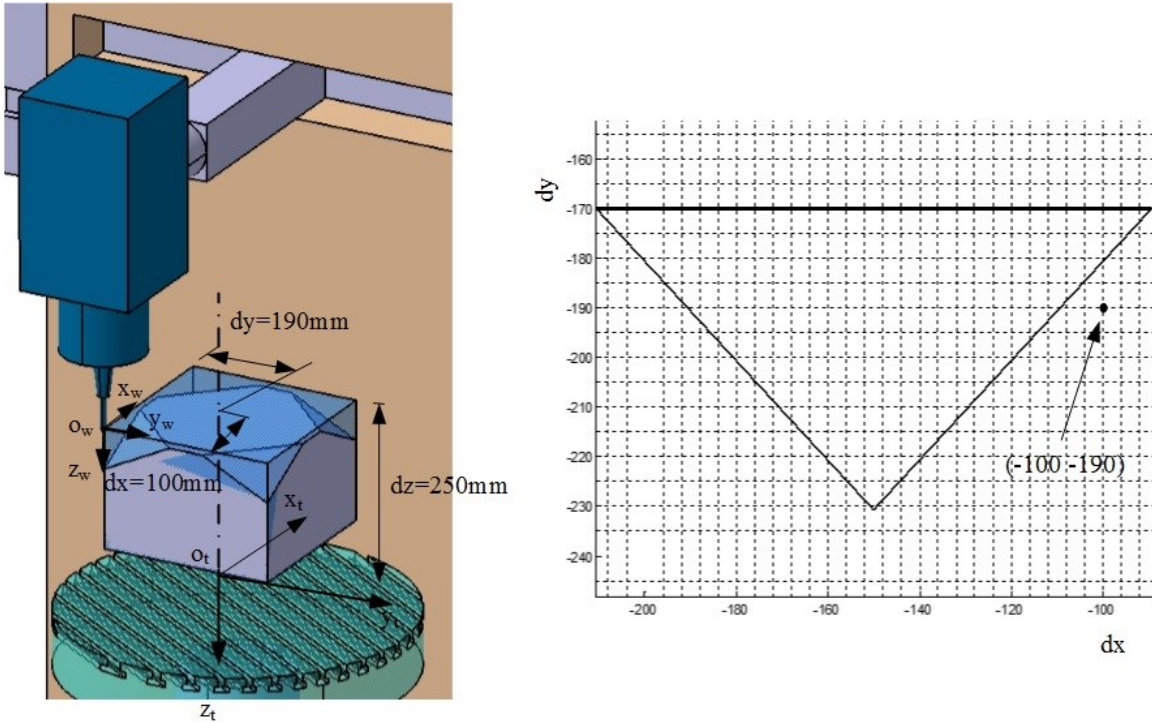


Figure 4.21- Infeasible setup of the part on the machine table along with the location of the feasible point outside the final feasible region.

### 4.5.3 Machining of the ‘bracket for holding the pipe’

To show the effectiveness of the method, machining of a practical part which includes several machining processes will be presented. The design part as shown in figure 4.22 includes some features which can be machined with the 5-axis continuous machining.

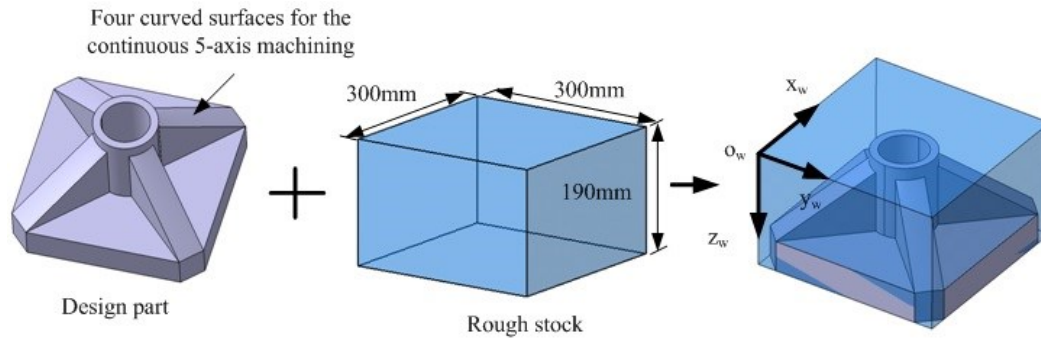


Figure 4.22-Design part (bracket for holding the pipe) and the rough stock.

For machining the part, following five machining operations are applied. The snapshots of these five machining operations are shown in figures 4.23 and 4.24.

- 1- Facing of the horizontal surface.
- 2- Pocketing of the four bottom faces with three levels of passes
- 3- Multi axis machining of curved surfaces of the four inclined rib supports with two level of passes. During the multi axis machining, tool axis is always normal to the drive surface.
- 4- Profile contouring of outer top circular face of the hole and four corner edges.
- 5- Internal pocketing of the hole followed by the drilling operation.

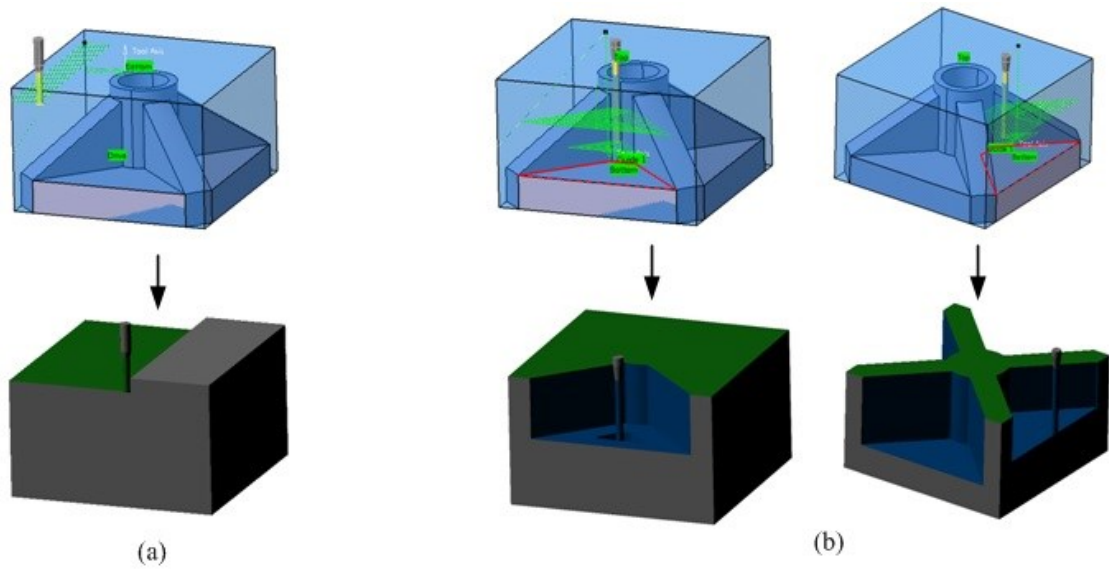
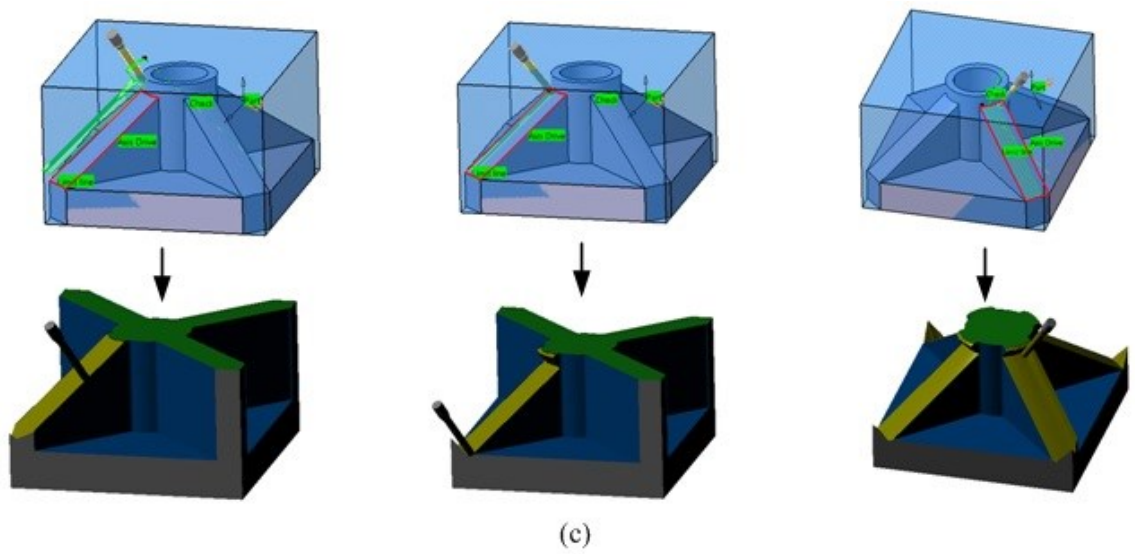


Figure 4.23- (a) Top surface facing (b) Pocketing of the four open islands (bottom faces) with three passes



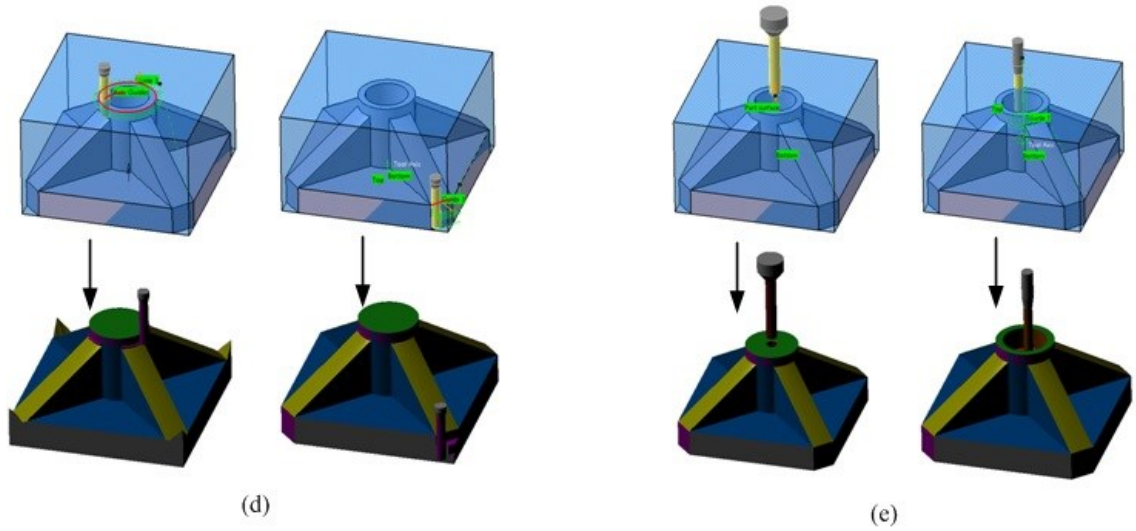


Figure 4.24- (Snap shot contd.): (c) Five axis continuous machining of the top surface of the four supporting ribs with two levels (d) Profile contouring of the cylindrical surface and four edges (e) Drilling and internal pocketing

After generating the tool path, it is necessary to find the feasible setup parameters before post processing (G-codes). For the complete machining of the above design part, feasible area for selecting the parameters 'dx' and 'dy' can be obtained by using the method developed in section 4.3.1. Figure 4.25 shows the common feasible area along with the feasible area of the different machining operations separately.

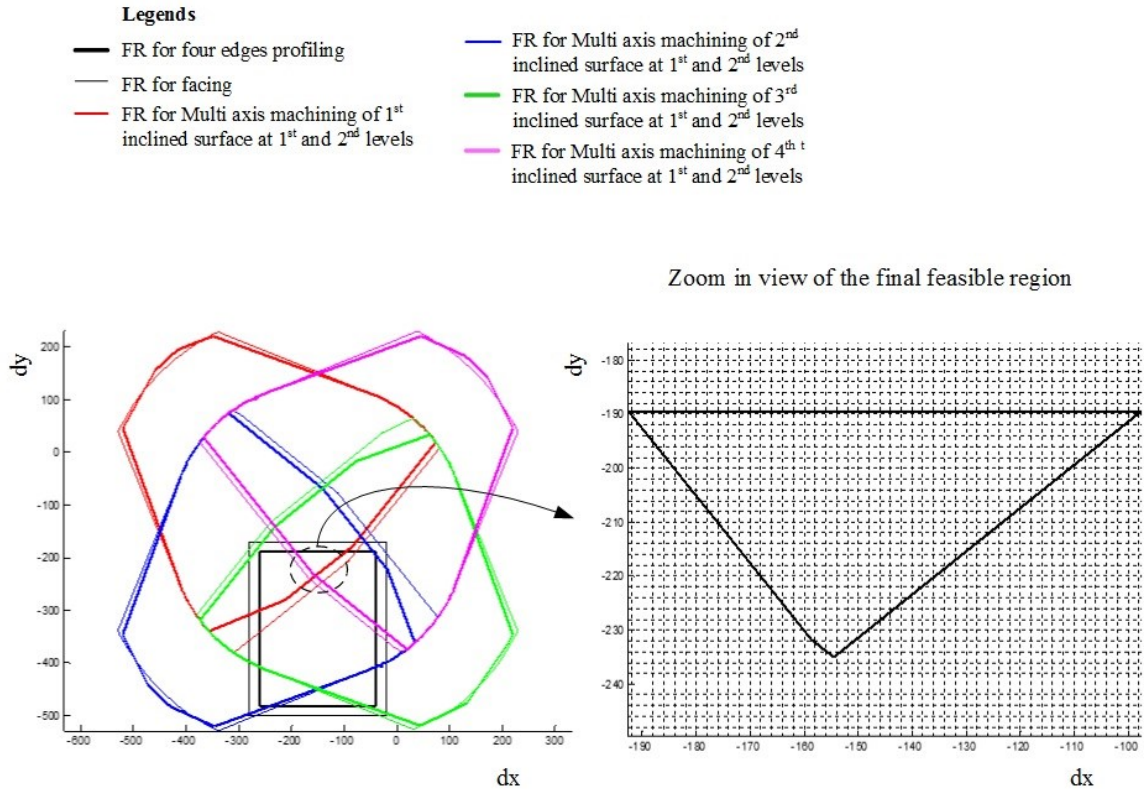


Figure 4.25- Common feasible region along with feasible regions for each machining operation.

The setup height parameter ‘dz’ should be selected in between the range, determined by the inequality (4.15) to avoid the z-over travel limit of the table. For the above example inequality (4.15) gives the result as

$$148.89 \leq dz \leq 464.72$$

Two setup parameters as shown in figure 4.26 are selected, one is the feasible and the other is not feasible. For the feasible and the infeasible setup parameters, coordinates of the ‘o<sub>w</sub>’ in the table coordinate system ‘o<sub>t</sub>’ are (-160 -200 -300) and (-180 -220 -300)

respectively. The machining simulation also shows that by choosing these setup parameters from infeasible region, complete machining of the part is not possible.

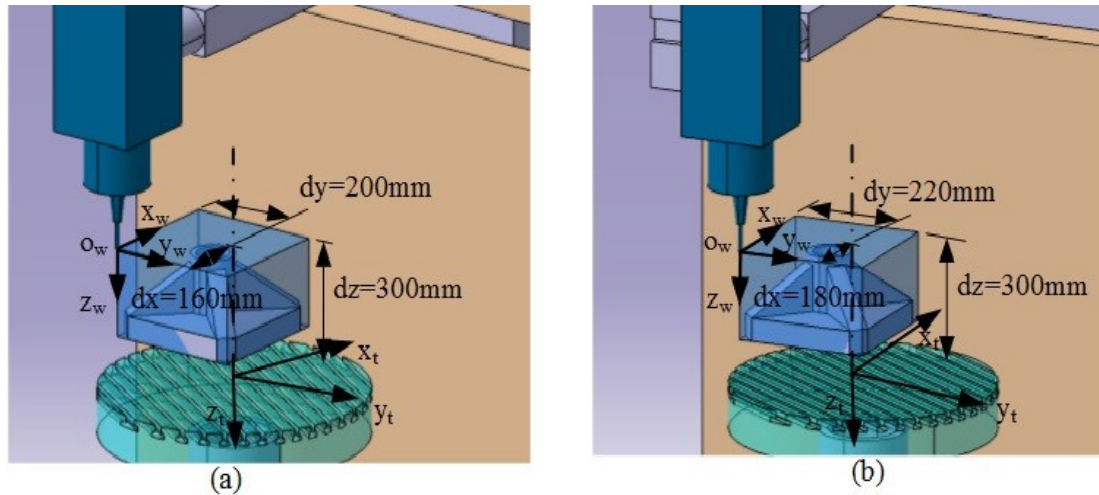


Figure 4.26- (a) Feasible setup of the rough stock. (b) Infeasible setup parameters of the rough stock.

#### 4.6 Summary

Fully utilization of the work space of the 5-axis machine tool is an important task, which is completely ignored by the previous researchers. Minimum number of the setup of the part improves efficiency of machining. The proposed algorithm has a capability of machining the bigger part on a small size five axis machine with the minimum number of setups.

The methodology developed in this chapter can be summarized as follow:

- 1 Development of the kinematic chain of the five axis machine tools along with the determination of the machine tool rotations from the tool vectors given in the part

coordinate system.

- 2 Determination of the tool tip and the table accessible work space in the table coordinate system based on the kinematics and the machine tool rotations.
- 3 From the kinematic chain and based on the setup parameters, determination of the cutter locations in the table coordinate system and bound these cutter locations within the tool tip and table accessible work space.
- 4 Solve the inequality functions formed due to the bounding of cutter locations within the tool tip and table accessible work space for the determination of the setup parameters.

## Chapter 5

### Conclusions and Future Work

In this dissertation two main and critical problems of five axis machining have been solved. The first contribution of this research is the comprehensive approach for the determination of the optimum cutter length for the five axis machining and the second contribution is the maximum utilization of the five axis machine useful workspace. The main contributions, which differs the present research work with the other researchers can be summarized as follows:

- 1 Consideration of the work in process model as a rough stock and representation of the work in process model as well as the fixture with the point cloud data. Representation of the solid surface with the point cloud data gives the flexibility of representing any type of fixture as well as any other moving part of the five axis machine tools.
- 2 An efficient way of confining the searching of the colloidal points among the point cloud data by using the KD tree data structure. No research has been conducted with this approach.
- 3 In industries different sizes of the tool holders are available. With the help of the algorithm of optimum tool length selection, selection of the tool holder is also possible, which gives the minimum overhang length of the cutter.

- 4 A new generic approach of the maximum utilization of the useful work space of the 5-axis machine tools is described. The key idea of this approach is the determination of the tool tip and the table accessible work space and based on these accessible work spaces, determination of the setup parameters.
- 5 This approach of selecting the work piece setup parameters gives the opportunity of selecting the minimum number of the setups of the part, which is required to do the complete machining of the part without reaching the over travel limits of the 5-axis machine tool translational axes.

For the future work, following topics are suggested:

- 1 Extension of the algorithm for the determination of the optimum cutter length for the other configuration of the five axis machine tools
- 2 The developed method is only for the collision detection at the CL points and there is also a possibility of collision at the interpolated points i.e. between the two consecutive cutter locations. Integration of the developed algorithm with some interpolation techniques to solve this issue.
- 3 The generic method developed for maximum utilization of the work space of five axis machine tools is only implemented for the five machines whose one rotary axis is located on the table, and the other is on the spindle. Implementation of this method is also possible for the other types of configuration.

## References

- [1] E.L.J. Bohez, "Five axis milling machine tool kinematic chain design and analysis." *International Journal of Machine Tools & Manufacture*, vol.42, pp.505-520, 2002.
- [2] K. Shirase, Y. Altintas, "Cutting force and dimensional surface error generation in peripheral milling with variable pitch helical end mills." *International Journal of Machine Tools and Manufacture*, vol. 36, pp.567-584, 1996.
- [3] G.M Kim, B.H. Kim, C.N. Chu, "Estimation of cutter deflection and form error in ball-end milling processes." *International Journal of Machine Tools and Manufacture*, vol. 43, pp.917-924, 2003.
- [4] L.N. L'opez de Lacalle, A. Lamikiz, J.A. S'anchez, M.A. Salgado, "Effects of tool deflection in the high-speed milling of inclined surfaces" *International Journal of Advanced Manufacturing Technology*, vol. 24, pp.621-631, 2004.
- [5] Y.S. Lee, "Admissible tool orientation control of gouging avoidance for 5-axis complex surface machining." *Computer Aided Design*, vol. 30, pp. 559-570, 1998.
- [6] C.C. Lo, "Efficient cutter-path planning for five axis surface machining with a flat-end cutter." *Computer Aided Design*, vol. 31, pp.557-566, 1999.
- [7] P.Gray, S.Bedi, F.Ismail, "Rolling ball method for 5-axis surface machining." *Computer Aided Design*, vol. 35, pp. 347-357, 2003.
- [8] P.Gray, S.Bedi, F.Ismail, "Arc-intersection method for 5-axis tool positioning." *Computer Aided Design*, vol. 37, pp. 663-674, 2005.
- [9] B.K. Choi, J.W. Part, C.S. Jun, "Cutter location data optimization in 5-axis surface machining." *Computer Aided Design*, vol. 25, pp. 377-386, 1993.
- [10] C.G. Jensen, W.E. Red, J. Pi, "Tool selection for five-axis curvature matched machining." *Computer Aided Design*, vol. 34, pp. 251-266, 2002.
- [11] M. Balasubramaniam, P. Laxmiprasad, S. Sarma, Z. Shaikh, "Generating 5-axis NC roughing paths directly from a tessellated representation." *Computer Aided Design*, vol. 32, pp. 261-277, 2000.
- [12] M. Balasubramaniam, S. Ho, S. Sarma, Y. Adachi, "Generation of collision free 5-axis tool paths using a haptic surface." *Computer Aided Design*, vol. 34, pp. 267-279, 2002.
- [13] M. Balasubramaniam, S. Sarma, K. Marciniak, "Collision free finishing tool paths from visibility data." *Computer Aided Design*, vol. 35, pp. 359-374, 2003.
- [14] S. Ho, S. Sarma, Y. Adachi, "Real time interference analysis between a tool and an environment." *Computer Aided Design*, vol. 33, pp. 935-947, 2001.
- [15] O. Illushin, G. Elber, D. Halperin, R.Wein, "Precise global collision detection in multi-axis NC- machining." *Computer Aided Design*, vol.37, pp. 909-920, 2005.

- [16] R.Wein, O. Illushin, G. Elber, D. Halperin, "Continuous path verification multi-axis machining." *International Journal of Computational Geometry & Applications*, vol.15, pp. 351-377, 2005.
- [17] B. Lauwers, P. Dejonghe, J.P. Kruth, "Optimal and collision free tool posture in five-axis machining through the tight integration of tool path generation and machine simulation." *Computer Aided Design*, vol.35, pp. 421-432, 2003.
- [18] H.T. Young, L.C. Chung, K. Gerschwiler, S. Kamps, "A five-axis rough machining approach for a centrifugal impeller." *International Journal of Advanced Manufacturing Technology*, vol. 23, pp.233-239, 2004.
- [19] R. Gian, T.W. Lin, A.C. Lin, "Planning of tool orientation for five axis cavity machining." *International Journal of Advanced Manufacturing Technology*, vol. 22, pp.150-160, 2003.
- [20] S.J. Kim, D.Y. Lee, H.C. Kim, S.G. Lee, M.Y. Yang, "CL surface deformation approach for a five-axis tool path generation." *International Journal of Advanced Manufacturing Technology*, vol. 28, pp.509-517, 2006.
- [21] M. Munlin, S.S.Makhanov, E.L.J.Bohez, "Optimization of rotations of a five-axis milling machine near stationary points." *Computer Aided Design*, vol.36, pp. 1117-1128, 2004.
- [22] Y.H. Jung, D.W. Lee, J.S. Kim, H.S. Mok, "NC postprocessor for 5-axis milling machine of table rotating/tilting type." *Journal of materials processing Technology*, vol. 130, pp.641-646, 2002.
- [23] Chen Liangi, "Kinematics modelling and post processing method of five axis CNC machine." First International Workshop on Education Technology and Computer Science, 2009.
- [24] A. Affouard, E. Duc, C. Lartigue, J.M. Langeron, P. Bourdet, "Avoiding 5-axis singularities using tool path deformation." *International Journal of Machine tool and Manufacture*, vol. 44, pp.415-425, 2004.
- [25] C.H.She, C.C.Chang, "Design of a generic five-axis postprocessor based on generalized kinematics model of machine tool." *International Journal of Machine tool and Manufacture*, vol. 47, pp.535-547, 2007.
- [26] W. Anotaipaiboon, S.S.Makhanov, E.L.J.Bohez, "Optimal setup for five-axis machining." *International Journal of Machine tool and Manufacture*, vol. 46, pp.964-977, 2006.
- [27] S.M. Stanislav, A. Weerachai, "Advance numerical method to optimize cutting operations of Five-axis milling machines." Springer-Verlag Berlin Heidelberg 2007.
- [28] T.D. Tang, E.L.J. Bohez, P. Koomsap, "The sweep plan algorithm for global collision detection with work piece geometry update for five-axis NC machining." *Computer Aided Design*, vol.39, pp. 1012-1024, 2007.
- [29] G. Turk, "Generating random points in triangles" In: Glassner AS, editor. *Graphic Gems*. Academic Press, 1990.

- [30] O. Robert, F. Thomas, C. Bernard, D. David, "Shape distributions" *ACM transactions on graphics*, vol.21, pp. 807-832, 2002.
- [31] J.L. Bentley, "Multidimensional binary search trees used for associative search." *Communication of the Association for Computing Machinery*, vol.18, pp. 509-517, 1975.
- [32] R.A. Finkel, J.L. Bentley, "Quad trees- A data structure for retrieval of composite keys." *Acta Informatica*, vol.4, 1974.
- [33] J.B. Rosenberg, "A study of data structures supporting region queries." *IEEE Transactions of Computer Aided Design*, vol.4, pp. 53-67, 1985.
- [34] S. Ding, M.A. Mannan, A.N. Poo, "Oriented bounding box and octree based global interference detection in 5-axis machining of free-form surfaces." *Computer Aided Design*, vol.36, pp. 1281-1294, 2004.
- [35] J.S.Arora, "Introduction to optimum design." 3<sup>rd</sup> edition, 2012 Elsevier Inc. USA
- [36] J.J. Craig, "Introduction to robotic mechanics and control." Pearson Education Inc. 2005.
- [37] L.Zhang, M. Yue, "Collision-free tool path generation for five-axis high speed machining." *Key Engineering Materials*, Vols.474-476, pp961-966, 2011



Tool path is generated in part coordinate system ( $O_w$ ) or Cutter locations and orientations are given in part coordinate system. Initially, origin of the cutter coordinate system coincides with the origin of the part coordinate system at machining zero point i.e all machine axis motions are set to zero. All reference coordinate systems are right handed coordinate system. For the standard set up of the work piece, orientation of the work piece coordinate system is same as the orientation of the coordinate system attached at the center of the table.

Let “ $P_w$ ”  $[CL_x \quad CL_y \quad CL_z \quad 1]^T$  be a point in the part coordinate system.

Following steps are needed to transform “ $P_w$ ” from the part coordinate system ( $o_w$ ) to the cutter coordinate system ( $o_c$ ).

**Step 1:**

Map the point ‘ $P_w$ ’ in the  $o_t$ -coordinate system.

$$P_t = T_1.P_w = \begin{bmatrix} 1 & 0 & 0 & dx \\ 0 & 1 & 0 & dy \\ 0 & 0 & 1 & dz \\ 0 & 0 & 0 & 1 \end{bmatrix} . P_w$$

Where  $(dx \quad dy \quad dz)$  are the coordinates of the ‘ $o_w$ ’ in the  $o_t$ -coordinate system and are called the setup parameters for mounting the work piece on the table.

**Step 2:**

Rotation around the  $z_t$ -axis in ‘ $o_t$ ’ by the angle ‘ $C$ ’.The point ‘ $P_t$ ’ is rotated around the  $z_t$ -axis in the  $o_t$ -coordinate system to a new location ‘ $P_t'$ ’.

$$P'_t = T_2 \cdot P_t = \begin{bmatrix} \cos C & -\sin C & 0 & 0 \\ \sin C & \cos C & 0 & 0 \\ 0 & 0 & 1 & 0 \\ 0 & 0 & 0 & 1 \end{bmatrix} \cdot P_t$$

**Step 3:**

Before translating the point  $P'_t$  in the  $o_p$ -coordinate system, it is necessary to transform the point  $P'_t$  in the other coordinate system ' $o_1$ ' which has the same origin as the  $o_t$ - coordinate system and has an orientation of the  $o_p$ -coordinate system.

$$P''_t = T_3 \cdot P'_t = \begin{bmatrix} 0 & 1 & 0 & 0 \\ 1 & 0 & 0 & 0 \\ 0 & 0 & -1 & 0 \\ 0 & 0 & 0 & 1 \end{bmatrix} \cdot P'_t$$

**Step 4:**

Translate the point ' $P''_t$ ' in the  $o_p$ -coordinate system with the machine slide translation ' $M$ '. The work piece attached to the table will appear to move away from the spindle in the negative directions of the  $o_p$ -coordinate system for the positive value of the machine slide translation ' $M$ '. Thus for machines slide translation  $M(x \ y \ Z)$ , the center of the  $o_1$ -coordinate system will be at the location of  $(-dx - x \ -dy - y \ -L_o + dz - Z)$  in the  $o_p$ -coordinate system.

$$P_p = T_6 \cdot P''_t = \begin{bmatrix} 1 & 0 & 0 & -dx - x \\ 0 & 1 & 0 & -dy - y \\ 0 & 0 & 1 & -L_o + dz - Z \\ 0 & 0 & 0 & 1 \end{bmatrix} \cdot P''_t$$

Where  $(-dx \quad -dy \quad -L_o + dz)$  is the coordinate of the origin 'o<sub>1</sub>' in the o<sub>p</sub>-coordinate system with respect to the machining zero position.

**Step 5:**

Rotation around the y<sub>p</sub>-axis in the o<sub>p</sub>-coordinate system by the angle 'b'. The point 'P<sub>p</sub>' is represented in the rotated coordinate system as a point P'<sub>p</sub>.

$$P'_p = T_5 \cdot P_p = \begin{bmatrix} \cos b & 0 & -\sin b & 0 \\ 0 & 1 & 0 & 0 \\ \sin b & 0 & \cos b & 0 \\ 0 & 0 & 0 & 1 \end{bmatrix} \cdot P_p$$

**Step 6:**

Map the point P'<sub>p</sub> in the cutter coordinate system 'o<sub>c</sub>'.

$$P_c = T_6 \cdot P'_p = \begin{bmatrix} 1 & 0 & 0 & 0 \\ 0 & 1 & 0 & 0 \\ 0 & 0 & 1 & L_o \\ 0 & 0 & 0 & 1 \end{bmatrix} \cdot P'_p$$

It is clear from the above steps; any point in the part coordinate system can be transformed in the cutter coordinate system by the following series of the transformations.

$$P_c = T_6 \cdot T_5 \cdot T_4 \cdot T_3 \cdot T_2 \cdot T_1 \cdot P_w$$

$$P_c = T_c^w \cdot P_w$$

After simplification, homogenous transformation matrix from work piece coordinate system to cutter coordinate system can be given as

$$T_c^w = \begin{bmatrix} \cos(b) \cdot \sin(C) & \cos(b) \cdot \cos(C) & \sin(b) & 0 \\ \cos(C) & -\sin(C) & 0 & 0 \\ \sin(b) \cdot \sin(C) & \cos(C) \cdot \sin(b) & -\cos(b) & 0 \\ 0 & 0 & 0 & 0 \\ \cos(b) \cdot [dx \cdot \sin(C) + dy \cdot \cos(C) - dx - x] - \sin(b) \cdot (Z - L_o) & & & \\ dx \cdot \cos(C) - dy \cdot \sin(C) - dy - y & & & \\ \sin(b) \cdot [dx \cdot \sin(C) + dy \cdot \cos(C) - dx - x] + \cos(b) \cdot (Z - L_o) & & & \\ & & & 1 \end{bmatrix}$$

Homogenous transformation matrix from cutter to work piece coordinate system is given as

$$T_w^c = (T_c^w)^{-1}$$

By knowing the coordinate of the origin (CL point) of the cutter coordinate system in the work piece coordinate system, it is easy to get the inverse of  $T_c^w$ . By taking the transpose of rotational part of  $T_{cutter}^w$  [36], we can calculate the inverse of  $T_c^w$  as

$$T_w^c = \begin{bmatrix} \cos(b) \cdot \sin(C) & \cos(C) & \sin(b) \cdot \sin(C) & CL_x \\ \cos(b) \cdot \cos(C) & -\sin(C) & \cos(C) \cdot \sin(b) & CL_y \\ \sin(b) & 0 & -\cos(b) & CL_z \\ 0 & 0 & 0 & 1 \end{bmatrix}$$

**A.2: Machine rotations (C and b) solutions for the given tool orientations**

For the possible rotation angles, we will discuss two cases

**(a) When the tool in the spindle rotate in positive direction**

To align the tool vector “I” with the  $y_w z_w$ -plane and for the positive tool rotation ‘b’, the table can be rotate by angle ‘C’ in the positive direction as well as in the negative direction.

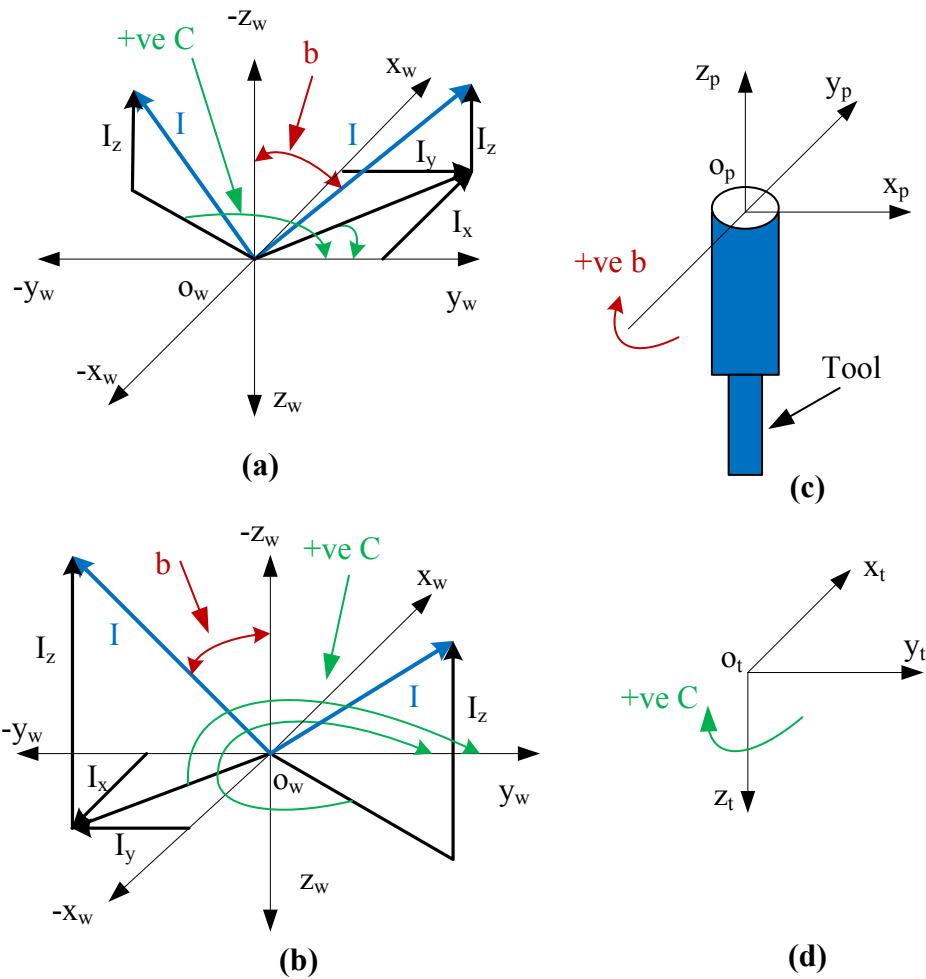


Figure A2- (a) & (b) Positive rotation of the table ‘C’ for positive rotation of spindle ‘b’, when tool vector is in different quadrants. (c) & (d) Spindle and table coordinate systems respectively with rotation directions

From figure A2;

$$\left. \begin{aligned}
 & \tan^{-1}\left(\frac{I_x}{I_y}\right) && I_x \geq 0, I_y > 0 \quad ; \text{For 1st quadrant. It also covers } C_1 = 0 \\
 & \frac{\pi}{2} && I_x > 0, I_y = 0 \quad ; \text{When tool vector is in } x_w z_w \text{-plane.} \\
 C_1 = & \tan^{-1}\left(\frac{I_x}{I_y}\right) + \pi && I_y < 0 \quad ; \text{For 2nd and 3rd quadrants.} \\
 & \tan^{-1}\left(\frac{I_x}{I_y}\right) + 2\pi && \text{otherwise} \quad ; \text{For 4th quadrant. It also covers, when} \\
 & && I_x < 0 \ \& \ I_y = 0 \ \text{i.e } \tan^{-1}\left(\frac{I_x}{I_y}\right) + 2\pi = \frac{3\pi}{2}
 \end{aligned} \right\}$$

$$b_1 = \cos^{-1}(-I_z) \quad (0 \leq b_1 \leq \theta_1)$$

Above equations give the positive rotation angle ‘ $C_1$ ’ when the tool vectors are in different quadrants. It is clear from figures (A2) (a) & (b) that by subtracting  $2\pi$  from the angle  $C_1$ , we can get the negative rotation of the table which also satisfied with the positive rotation of the spindle.

$$C'_1 = C_1 - 2\pi \quad \text{and} \quad b_1 = \cos^{-1}(-I_z) \quad (0 \leq b_1 \leq \theta_1)$$

Therefore,  $(C_1, b_1)$  and  $(C'_1, b_1)$  are the two possible solutions of the rotation required to align the tool in the spindle with the tool vector in the part coordinate system.

**(b) When the tool in the spindle rotate in negative direction**

To align the vector “I” with the  $y_w z_w$ -plane and for the negative tool rotation ‘b’, the table can be rotate by the angle ‘C’ in the positive direction as well as in the negative direction.

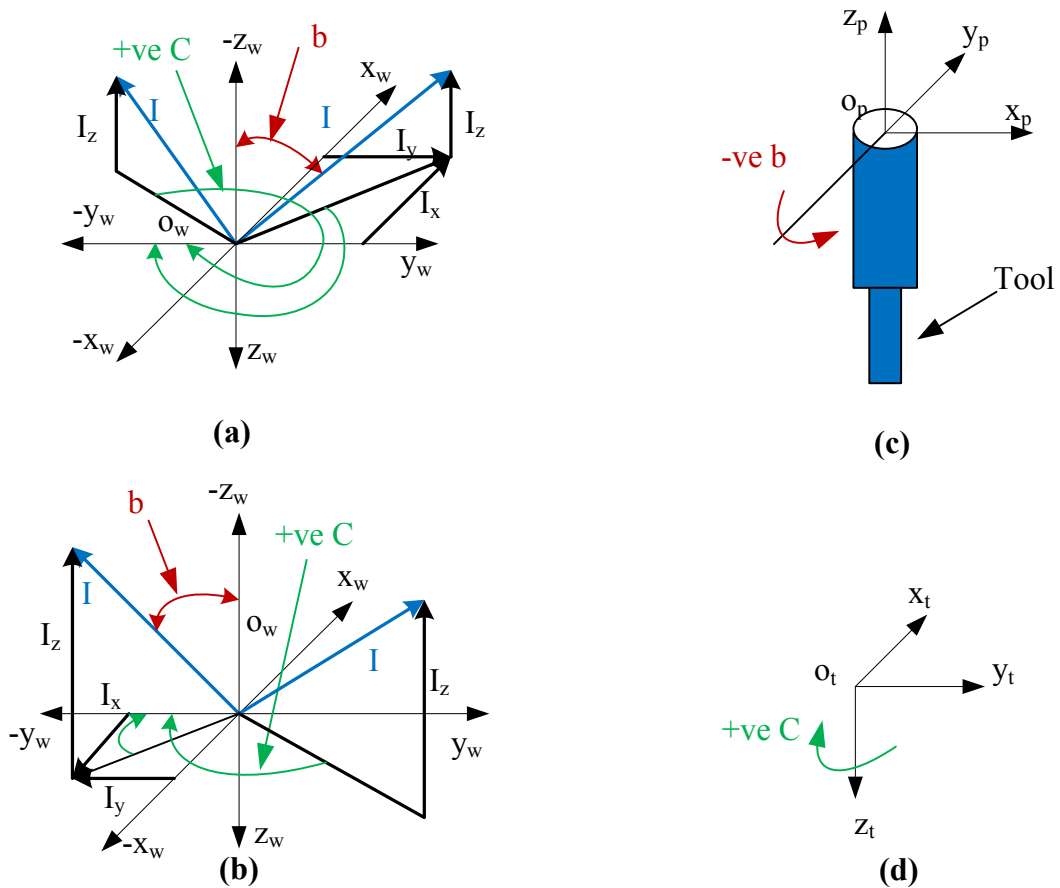


Figure A3- (a) & (b) Positive rotation of the table for the negative rotation of ‘b’ when the tool vector is in different quadrants. (c) & (d) Spindle and the table coordinate systems respectively with the rotation direction.

From figure (A3)

$$\left. \begin{array}{l}
 \tan^{-1}\left(\frac{I_x}{I_y}\right) \quad I_x \leq 0, \quad I_y < 0 \quad ; \text{ For 3rd quadrant. It also covers } C_2 = 0 \\
 \frac{\pi}{2} \quad I_x < 0, \quad I_y = 0 \\
 C_2 = \tan^{-1}\left(\frac{I_x}{I_y}\right) + \pi \quad I_y > 0 \quad ; \text{ For 1st and 4th quadrants.} \\
 \tan^{-1}\left(\frac{I_x}{I_y}\right) + 2\pi \quad I_x > 0, \quad I_y < 0 \quad ; \text{ For 2nd quadrant.} \\
 \frac{3\pi}{2} \quad I_x > 0, \quad I_y = 0
 \end{array} \right\}$$

$$b_2 = -\cos^{-1}(-I_z) \quad (\theta_2 \leq b_2 \leq 0)$$

Above equations give the positive rotation angle ‘ $C_2$ ’ when the tool vectors are in the different quadrants. It is clear from figures (A3) (a) & (b), that by subtracting  $2\pi$  from the angle  $C_2$ , we can get the negative rotation of the table which also satisfied with the negative rotation of the spindle.

$$C'_2 = C_2 - 2\pi \quad \text{and} \quad b_2 = -\cos^{-1}(-I_z) \quad (\theta_2 \leq b_2 \leq 0)$$

Therefore  $(C_2, b_2)$  and  $(C'_2, b_2)$  are the other two possible solutions of rotation required to align the tool in the spindle with the tool vector in part coordinate system.